NASA TECHNICAL NOTE

NASA TN D-6911

NASA TN D-6911

STRUCTURE OF ZIRCONIUM-93 AND ZIRCONIUM-91 AS SHOWN BY THE REACTIONS $^{92}Zr(d,p)^{93}Zr$ AND $^{92}Zr(d,t)^{91}Zr$

by Norton Baron, Regis F. Leonard, William M. Stewart, Charles L. Fink, Per Rex Christensen, Jerry Nickles, and Tor F. Thorsteinsen

Lewis Research Center
Cleveland, Ohio 44135

NATIONAL AERONAUTICS AND SPACE ADMINISTRATION • WASHINGTON, D. C. • SEPTEMBER 1972

1. Report No.	2. Government Accession No.	3. Recipient's Catalog No.
NASA TN D-6911		

4. Title and Subtitle	5. Report Date
STRUCTURE OF ZIRCONIUM-93 AND ZIRCONIUM-91 AS SHOWN BY THE REACTIONS $^{92}Zr(d,p)^{93}Zr$ AND $^{92}Zr(d,t)^{91}Zr$	September 1972
	6. Performing Organization Code

7. Author(s)	8. Performing Organization Report No.
Norton Baron, Regis F. Leonard, and William M. Stewart, Lewis Research Center; Charles L. Fink, Argonne National Laboratory; Per Rex Christensen, Niels Bohr Institute; Jerry Nickles, U. of Wisconsin; and Tor F. Thorsteinsen, U. of Bergen	E-6738
	10. Work Unit No. 112-02

9. Performing Organization Name and Address	11. Contract or Grant No.
Lewis Research Center National Aeronautics and Space Administration Cleveland, Ohio 44135	
	13. Type of Report and Period Covered
12. Sponsoring Agency Name and Address	Technical Note
National Aeronautics and Space Administration Washington, D. C. 20546	14. Sponsoring Agency Code

15. Supplementary Notes

16. Abstract

Deuterons of 13-MeV incident energy were scattered from ^{92}Zr. The $^{92}Zr(d,p)^{93}Zr$ data analysis resulted in the location of 47 levels up to an excitation energy of 4.84 MeV, and the spins of 43 of these levels were identified. Essentially all the strength of the $2d_{5/2}$, $3s_{1/2}$, $2d_{3/2}$, and $1g_{7/2}$ shells was observed; and the excitation energy of their centroids was computed to be 0.00, 1.21, 2.23, and 2.37 MeV, respectively. We also observed 43 percent of the $1h_{11/2}$ strength, 21 percent of the $2f_{7/2}$ strength, and 3 percent of the $3p_{3/2}$ strength. In addition, the $^{92}Zr(d,t)^{91}Zr$ data analysis resulted in the location of 26 levels up to an excitation energy of 4.01 MeV, and the spins of 21 of these levels were identified. We obtained most of the expected strength of the $2d_{5/2}$ and $1g_{9/2}$ shells; and the excitation energy of their centroids was computed to be 0.31 and 3.19 MeV, respectively. In addition, six $l=1$ states are populated belonging to either the $2p_{1/2}$ or $2p_{3/2}$ shells.

17. Key Words (Suggested by Author(s))	18. Distribution Statement
Nuclear spectroscopy, direct reaction, zirconium, $^{92}Zr(d,p)^{93}Zr$, $^{92}Zr(d,t)^{91}Zr$	Unclassified - unlimited

19. Security Classif. (of this report)	20. Security Classif. (of this page)	21. No. of Pages	22. Price*
Unclassified	Unclassified	58	$3.00

* For sale by the National Technical Information Service, Springfield, Virginia 22151

STRUCTURE OF ZIRCONIUM-93 AND ZIRCONIUM-91 AS SHOWN BY THE REACTIONS $^{92}Zr(d,p)^{93}Zr$ AND $^{92}Zr(d,t)^{91}Zr$

by Norton Baron, Regis F. Leonard, William M. Stewart, Charles L. Fink,* Per Rex Christensen,** Jerry Nickles,† and Tor F. Thorsteinsen‡

Lewis Research Center

SUMMARY

The structures of ^{93}Zr and ^{91}Zr were studied by means of the stripping reaction $^{92}Zr(d,p)^{93}Zr$ and the pickup reaction $^{92}Zr(d,t)^{91}Zr$ induced by 13-MeV incident deuterons.

The $^{92}Zr(d,p)^{93}Zr$ data analysis resulted in the location of 47 levels up to an excitation energy of 4.84 MeV. Parities and assumed spin assignments for 43 of these levels were made on the basis of direct single-particle reaction calculations, with distorted waves in the incident and exit channels, and shell model considerations. Essentially all the strength of the $2d_{5/2}$, $3s_{1/2}$, $2d_{3/2}$, and $1g_{7/2}$ shells was observed; and the excitation energy of their centroids was computed to be 0.00, 1.21, 2.23, and 2.37 MeV, respectively. Also observed were 43 percent of the $1h_{11/2}$ strength, 21 percent of the $2f_{7/2}$ strength, and 3 percent of the $3p_{3/2}$ strength.

The pickup reaction $^{92}Zr(d,t)^{91}Zr$ data analysis resulted in the location of 26 levels up to an excitation energy of 4.01 MeV. As for the (d,p) analysis, parities and assumed spin assignments for 21 of these levels were made on the basis of direct reaction calculations and shell model considerations. Most of the expected strength of the $2d_{5/2}$ and $1g_{9/2}$ shells was found, and the excitation energy of their centroids was computed to be 0.31 and 3.19 MeV, respectively. Of the six $l=1$ levels that were observed, each could have a spin and parity of either $1/2^-$ or $3/2^-$. It is likely that most of the lower lying $l=1$ levels are $1/2^-$ and will account for most of the expected strength. However, it is expected that one or more of the higher lying levels represent neutrons picked up from the $2p_{3/2}$ shell. In addition, levels at 1.196 MeV ($1/2^+$), 2.036 MeV ($3/2^+$), 2.186 MeV ($7/2^+$), and 3.314 MeV ($1/2^+$) are populated corresponding to pickup from single-particle shells which are nominally empty in ^{92}Zr.

---

*Argonne National Laboratory, Lamont, Illinois.

**Professor of Physics, Niels Bohr Institute, Copenhagen, Denmark.

†University of Wisconsin, Madison, Wisconsin.

‡Professor of Physics, University of Bergen, Bergen, Norway.

INTRODUCTION

This report presents the results of a study of the level structures of ^{93}Zr and ^{91}Zr made by using the reactions $^{92}Zr(d,p)^{93}Zr$ and $^{92}Zr(d,t)^{91}Zr$ induced by 13-MeV incident deuterons. Primarily, this work is intended as an extension of results of previous investigations (refs. 1 to 3) concerning the level structure of ^{93}Zr. But in this study better resolution and counting statistics resulted in many more levels observed in ^{93}Zr. In addition, although much work has been reported on the level structure of ^{91}Zr by means of the reaction mechanisms (d,p) (refs. 1, and 4 to 6), $(\alpha, ^3He)$ (ref. 4), $(\alpha, n\gamma)$ (ref. 7), (p,d) (ref. 8), and (p,p') (refs. 9 to 11), there has been no thorough (d,t) study leading to excited levels of ^{91}Zr. Since in this nucleus there is a single $2d_{5/2}$ neutron outside a closed shell of 50 neutrons, it is important to know its level structure well in order to understand the finer details of the single-neutron strength function. These previous studies of ^{91}Zr have shown that its structure deviates considerably from the single-particle model and is described to a considerable extent by particle-core coupling concepts. By comparing the complexity of the ^{93}Zr structure with that of ^{91}Zr, it is hoped that greater insight will be attained concerning the particle-core coupling processes involved for these isotopes.

In this report the experimental arrangement is described, and the procedures followed for reducing the data are explained. The experimental results are then presented and are interpreted on the basis of direct single-particle reaction calculations with distorted waves in the incident and exit channels. Next a brief qualitative discussion of the level structure in terms of the shell model and particle-core coupling scheme is presented. Some conclusions are drawn concerning the configuration of the observed excited levels of ^{93}Zr and ^{91}Zr, as well as the ground state of ^{92}Zr.

EXPERIMENTAL ARRANGEMENT

The structures of ^{93}Zr and ^{91}Zr were studied by means of the stripping reaction $^{92}Zr(d,p)^{93}Zr$ and the pickup reaction $^{92}Zr(d,t)^{91}Zr$ induced by 13-MeV incident deuterons. The experiment was performed at the tandem van de Graaf facilities of the Niels Bohr Institute of the University of Copenhagen and the University of Pittsburgh. Isotopically enriched ^{92}Zr targets having an areal density of 0.7 mg/cm^2 were used. The reaction product particles were detected by using a $\Delta E \times E$ counter telescope. The front transmission counter was a 51×10^{-4}-centimeter-thick silicon surface-barrier type. The rear stopping counter was a 3-millimeter-thick lithium-drifted silicon surface-barrier type. The solid angle subtended at the target by the counter telescope was 2.75×10^{-4} steradian.

In figure 1 is shown a block diagram of the electronic circuit used to process the detectors' output signals. The circuit was quite conventional. The ΔE and E signals were preamplified, amplified, stretched, and then fed into an identification circuit in order to discriminate between protons, deuterons, and tritons. The proper setting of the identifier single-channel analyzer window widths was facilitated by monitoring with a pulse height analyzer (PHA). The identifier outputs were then used to route the energy sum signals into their appropriate storage locations in a second PHA. The PHA had a

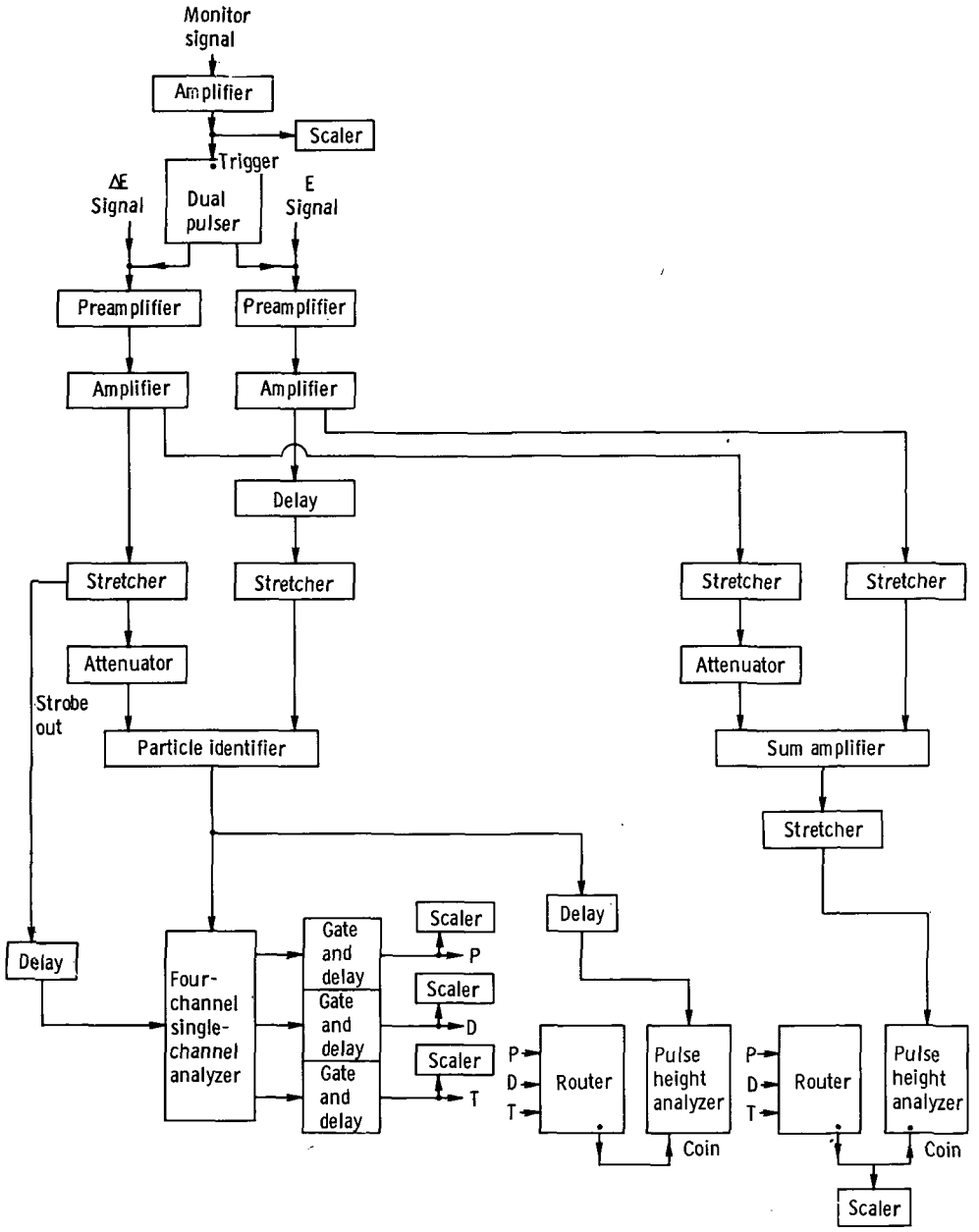

Figure 1. - Block diagram of electronic circuit.

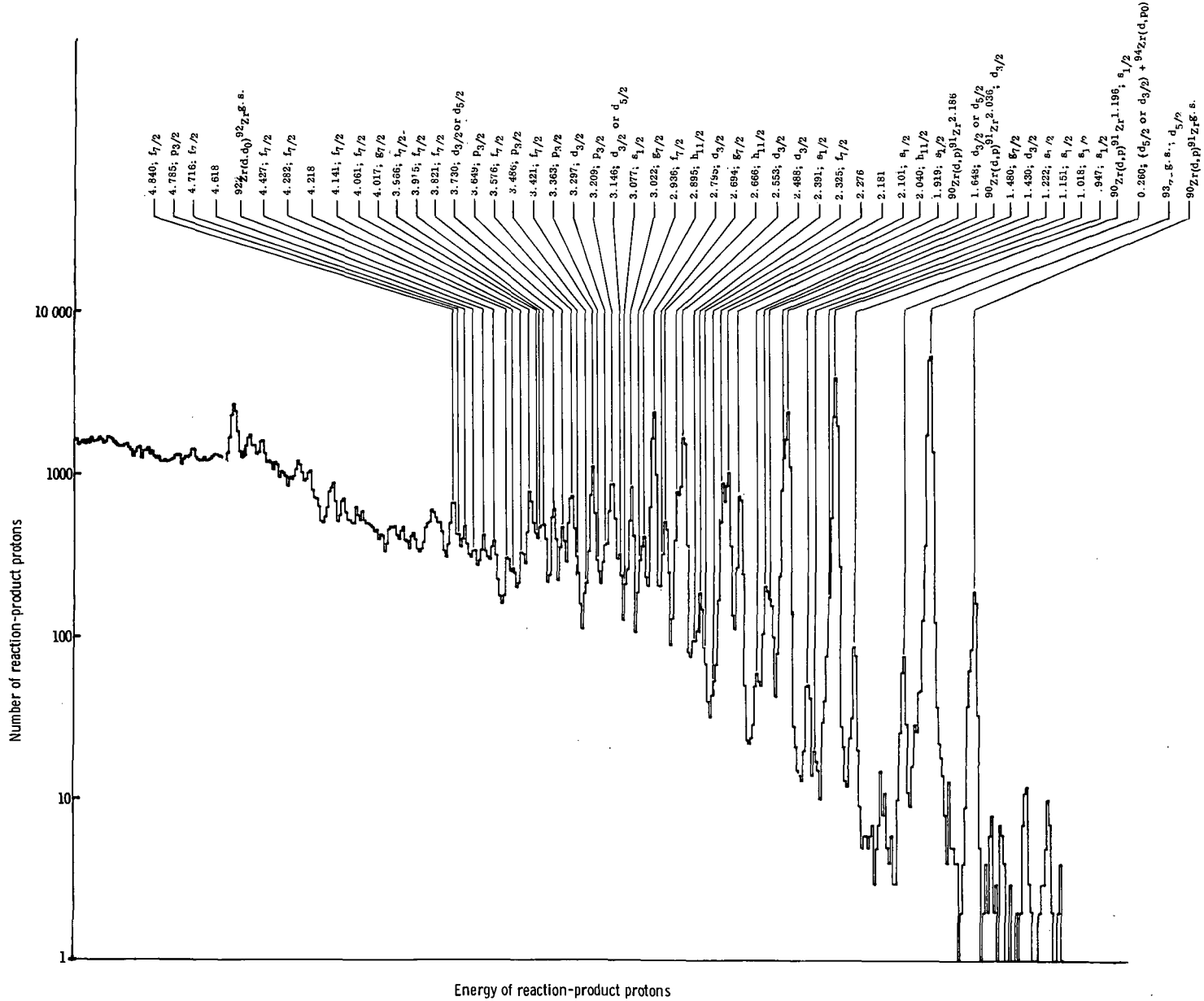

Figure 2. - $^{92}Zr(d,p)^{93}Zr$ spectrum. Laboratory scattering angle, 60^0.

4096-channel memory, and the energy sum signals of these three different types of particles were stored in different 1024-channel quadrants of the PHA. The stored data were then dumped onto magnetic tape to be used for subsequent off-line computer analysis.

REDUCTION OF DATA

Some typical spectra from the reactions $^{92}Zr(d,p)^{93}Zr$ and $^{92}Zr(d,t)^{91}Zr$ are pictured in figures 2 and 3, respectively. The overall experimental resolution was 35 to 45 keV.

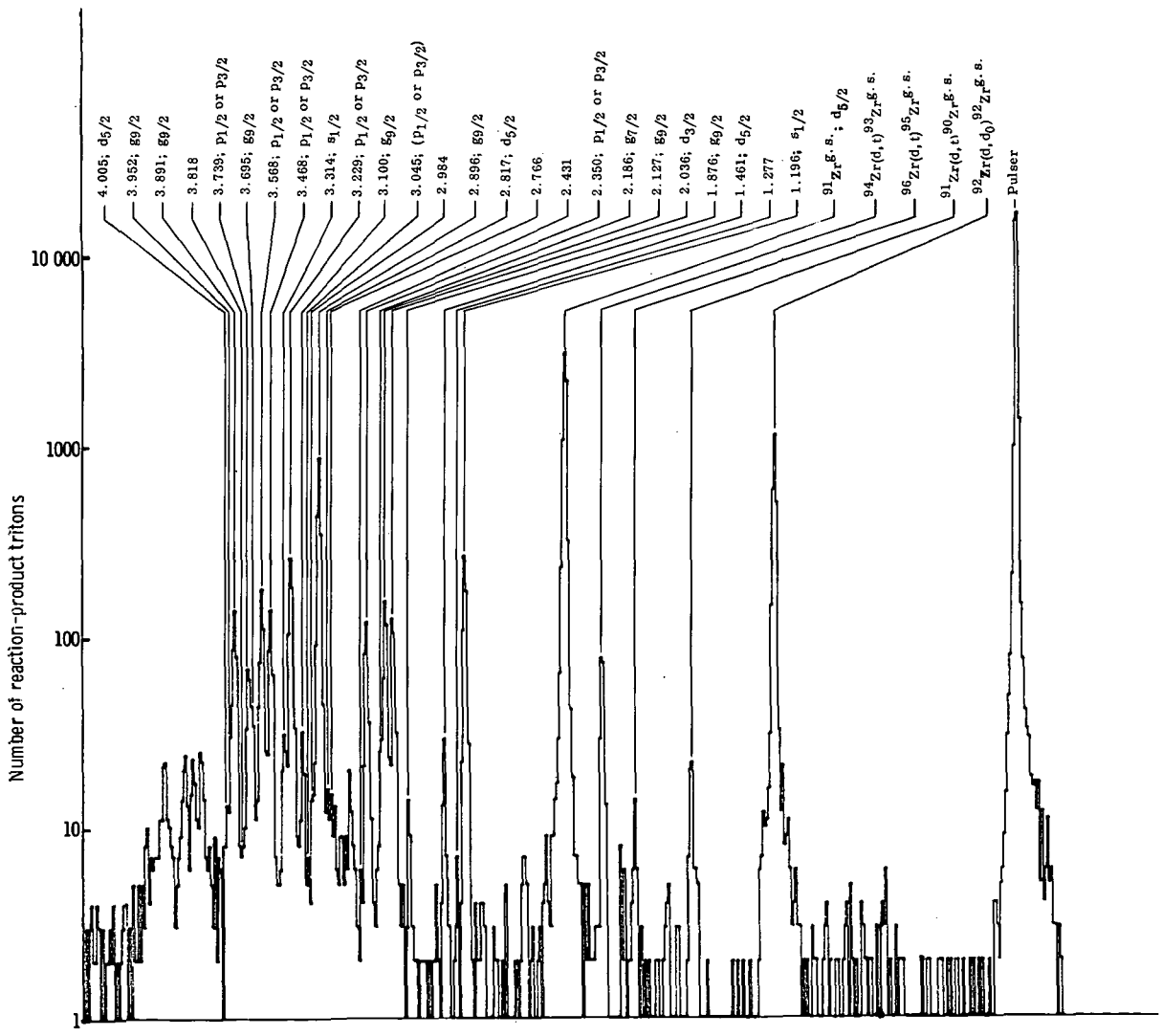

Figure 3. - $^{92}Zr(d,t)^{91}Zr$ spectrum. Laboratory scattering angle, 60^{o}.

Spectrum Stripping

Each spectrum was analyzed by a nonlinear least-squares peak-fitting program similar to one previously described (ref. 12). The background was also searched for.

Dead-Time Correction

The experimental arrangement used at the University of Pittsburgh included a dual pulser. Its outputs, which were adjusted to simulate a triton signal, were fed into the front ends of the ΔE and E preamplifiers; and the sum signal was collected in the triton portion of the PHA. The dual pulser was triggered by the monitor counter's output signal. The system dead-time was obtained by comparing the monitor (or pulser trigger) counts with the PHA stored pulser counts.

Isotopic Abundance of ^{92}Zr in Target

The target material used in this experiment was determined to have the relative composition listed in the following table. These values were calculated by comparing

Target	Isotopic enrichment, percent
^{90}Zr	2.3
^{91}Zr	2.1
^{92}Zr	93.8
^{94}Zr	1.6
^{96}Zr	.2

the yield of the reaction $^{90}Zr(d,p_0)^{91}Zr$ with that of $^{92}Zr(d,p_0)^{93}Zr$ (fig. 2) and the yields of the reactions $^{91}Zr(d,t_0)^{90}Zr$, $^{94}Zr(d,t_0)^{93}Zr$, and $^{96}Zr(d,t_0)^{95}Zr$ with that of the reaction $^{92}Zr(d,t_0)^{91}Zr$ (fig. 3). For these calculations, the reaction cross sections used were those predicted by a direct reaction calculation for single-particle excitation, wherein it was assumed that all the strength was in the ground state. The rela-

tive percentage composition of the target was computed by

$$\frac{(\rho t)^{^{90}Zr}}{(\rho t)^{target}} = \left[\frac{\left(\frac{d\sigma}{d\Omega}\right)^{^{92}Zr(d,p_0)^{93}Zr}_{calc}}{\left(\frac{d\sigma}{d\Omega}\right)^{^{90}Zr(d,p_0)^{91}Zr}_{calc}}\right]_\theta \left[\frac{(Yield)^{^{90}Zr(d,p_0)^{91}Zr}}{(Yield)^{^{92}Zr(d,p_0)^{93}Zr}}\right]_\theta, \text{ etc.}$$

Cross Sections

The absolute magnitudes of the cross sections were calculated by using the measured integrated incident charge, the solid angle, the dead-time correction, and the target thickness. It was estimated that the quoted absolute cross sections are uncertain by ±10 percent.

Determination of Excitation Energies

The dual pulser setting (fig. 1) was unchanged throughout the experiment, and its sum signal was observed to fall in the same PHA channel for all the runs. This provided evidence of no significant electronic drifts throughout the course of the experiment. Consequently, one linear energy calibration curve was generated by using the method of least squares to fit the ground-state centroids of the (d,p), (d,d), and (d,t) levels from all the experimental runs. Since the angular range of the measurements extended from 15° to 140°, the kinematic shift of these levels over this angular range resulted in many calibration points, which sufficiently covered the energy region of interest. From this calibration curve, excitation energies of the observed levels were obtained. The listed excitation energies of the observed levels are uncertain to ±10 keV.

EXPERIMENTAL RESULTS

Reaction $^{92}Zr(d, p)^{93}Zr$

Spectrum stripping of the (d,p) data resulted in the location of 47 levels up to an

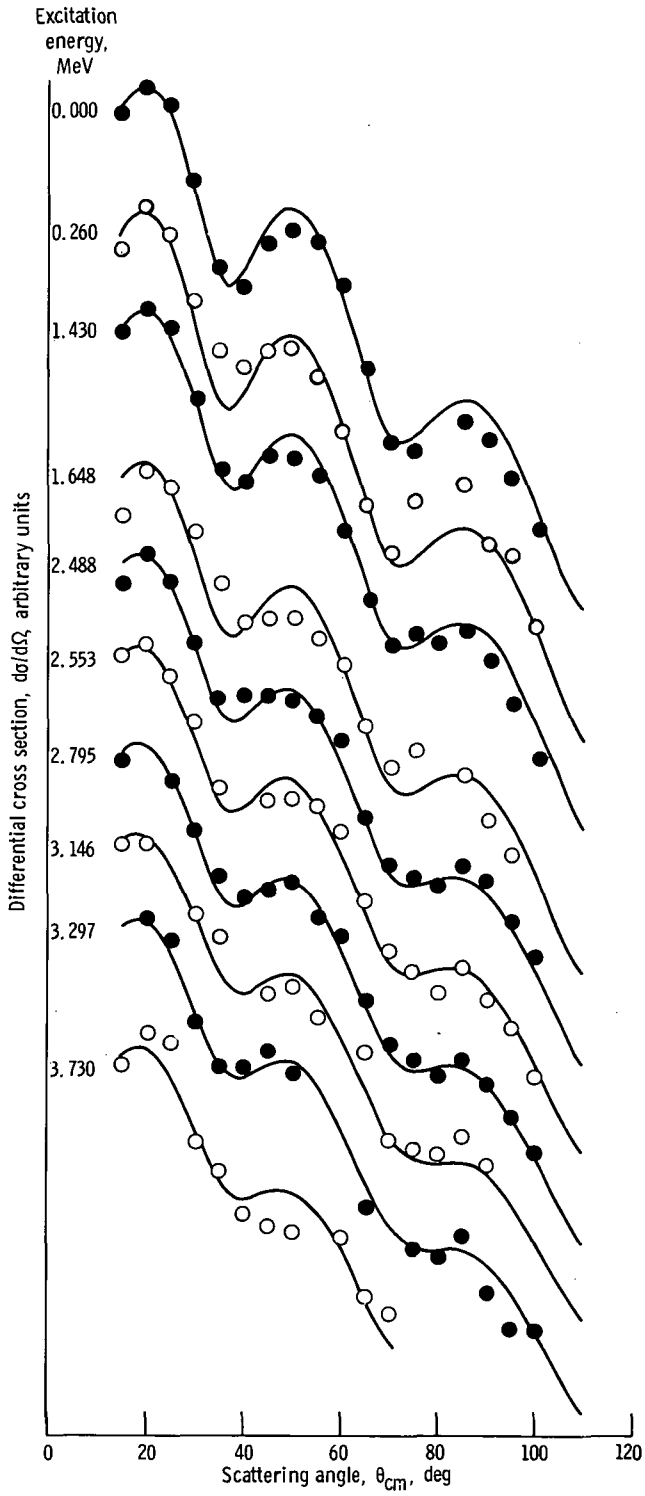

(a) Momentum transfer, 2.

Figure 4. - Comparison of experimental angular distributions with theoretical (DWBA) calculations for observed excited levels in ^{93}Zr induced by reaction $^{92}Zr(d, p)^{93}Zr$.

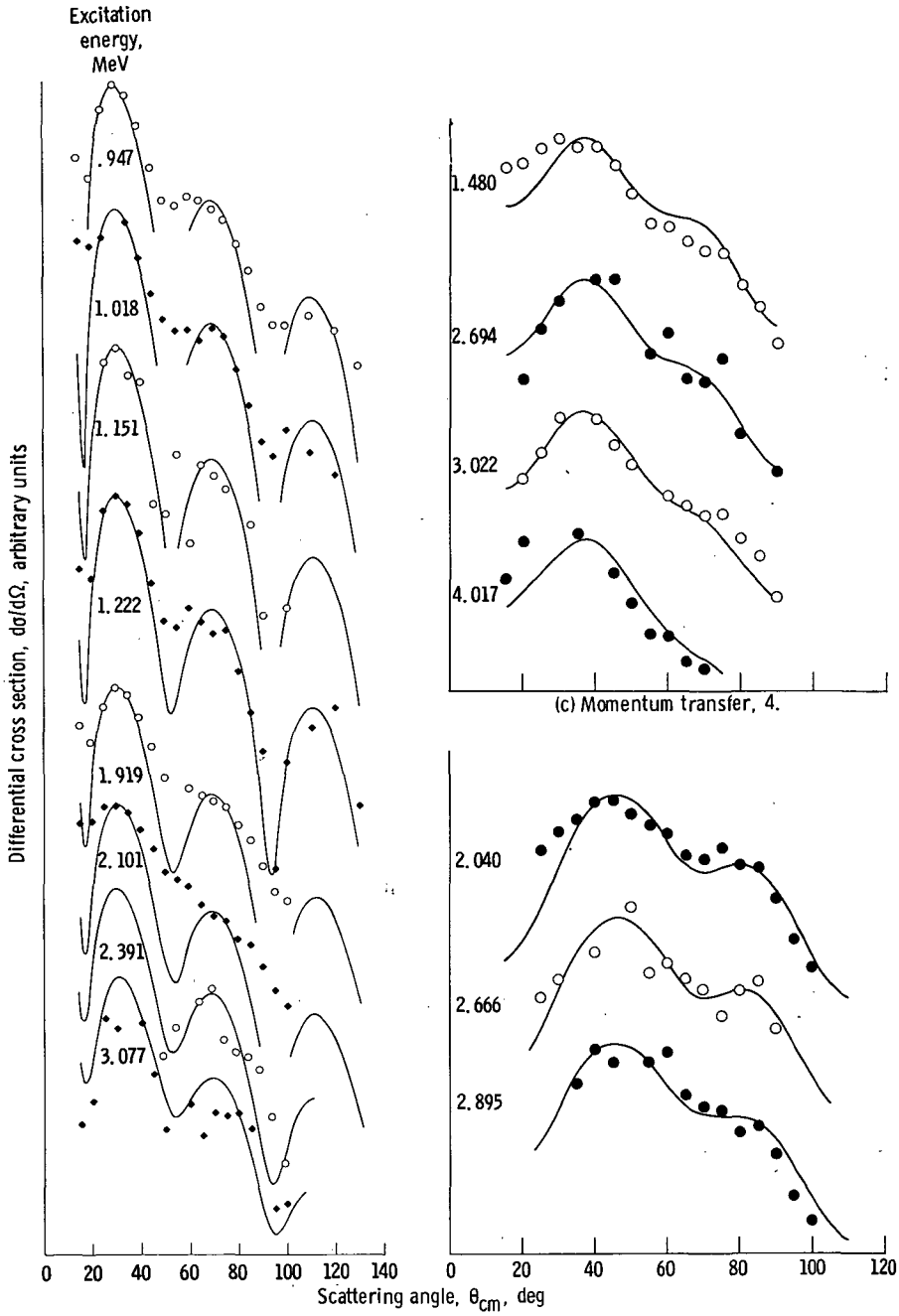

Figure 4. - Continued.

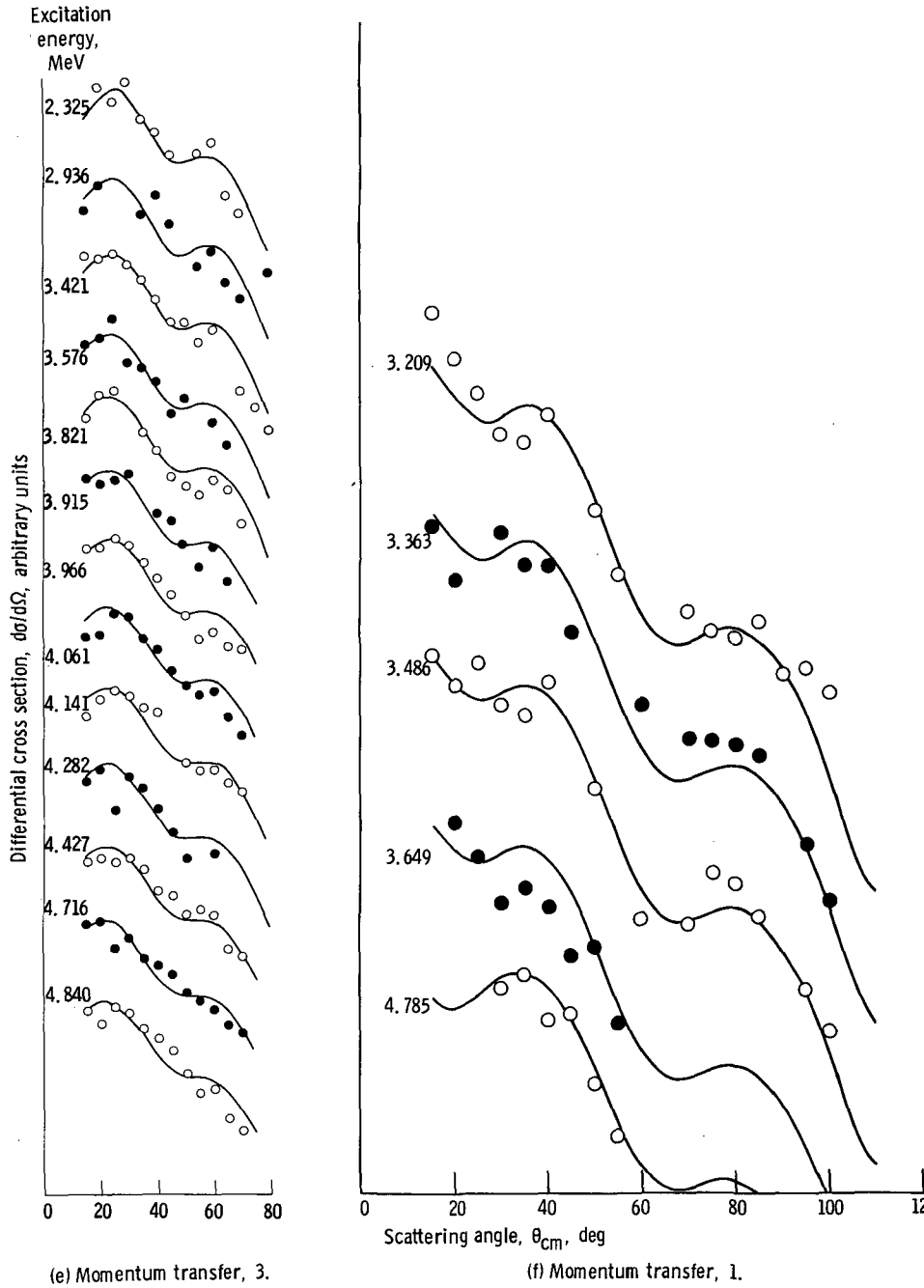

(e) Momentum transfer, 3.

(f) Momentum transfer, 1.

Figure 4. - Concluded.

excitation energy of 4.840 MeV in ^{93}Zr. The measured cross sections of 43 of these levels resulted in angular distributions that were analyzable. Tabulated in table I are the measured cross sections and excitation energies for each of the analyzable levels. The angular distributions are pictured in figure 4.

Reaction $^{92}Zr(d, t)^{91}Zr$

Spectrum stripping of the (d,t) data resulted in the location of 26 levels up to an

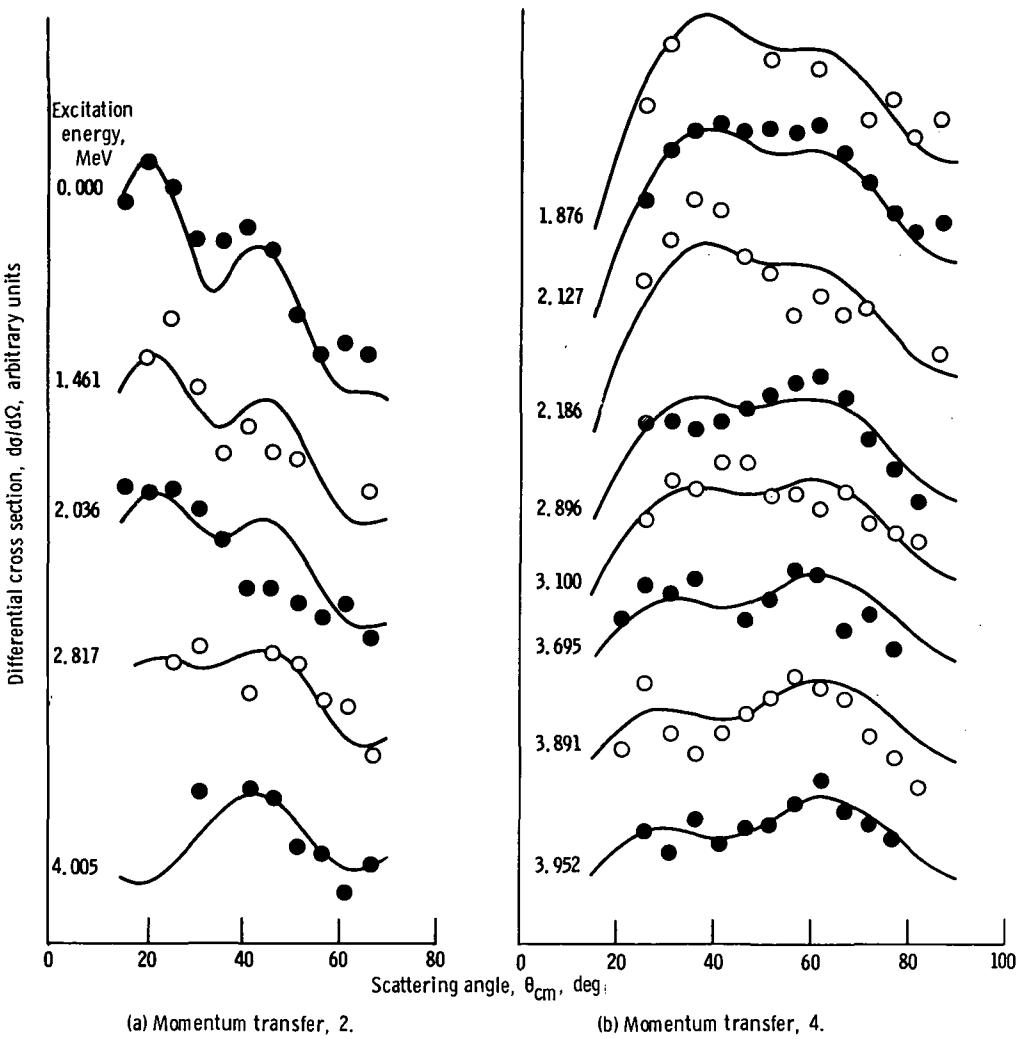

Figure 5. - Comparison of experimental angular distributions with theoretical (DWBA) calculations for observed excited levels of ^{91}Zr induced by reaction $^{92}Zr(d, t)^{91}Zr$.

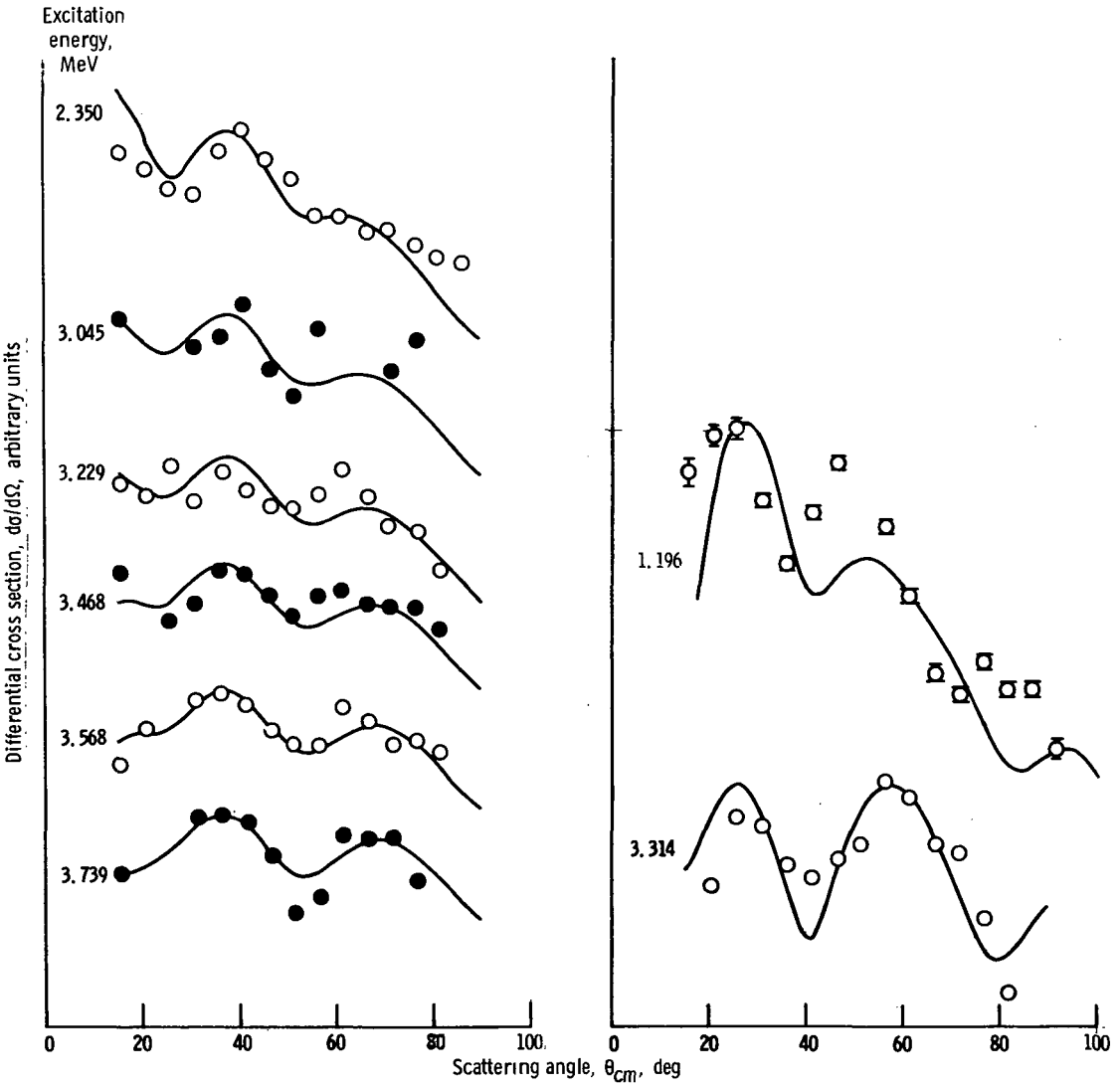

(c) Momentum transfer, 1.

(d) Momentum transfer, 0.

Figure 5. - Concluded.

excitation energy of 4.005 MeV in ^{91}Zr. The measured cross sections of 21 of these levels resulted in angular distributions that were analyzable. Tabulated in table II are the measured cross sections and excitation energies for each of the analyzable levels. The angular distributions are pictured in figure 5.

DESCRIPTION OF DISTORTED-WAVE-BORN-APPROXIMATION ANALYSIS FOR SINGLE-PARTICLE EXCITATION

Determination of Angular Momentum Transfers

The determination of the orbital angular momentum l of the transferred particle for each of the observed excited levels was made by determining which l-dependent calculated distribution agrees best with the experimental angular distribution. The calculation assumed a direct reaction process for excitation of single-particle states with distorted waves for the incident and exit channels. This distorted-wave-Born-approximation (DWBA) calculation was made by using the computer program DWUCK (private communication from P.D. Kunz). The number of partial waves used in these calculations was 25. The lower cutoff on the radial integrals was 0 fermi, and the upper cutoff was 80 fermis. Neither nonlocal nor finite range corrections were used.

Optical Potentials

Listed in table III are the optical potentials used in the DWBA calculations. Shown there are the bound-state potential, the proton optical potential (ref. 13), the triton optical potential (ref. 14), and the deuteron optical potential. The spin-orbit contribution to the proton potential (ref. 13) was not used herein since in several test cases it was found to be of little importance. The deuteron potential was calculated to reproduce the deuteron elastic cross sections that were measured in this experiment. The calculation was made by using the computer program SCATLE (ref. 15). The form of the potential chosen to fit the deuteron elastic data included a real central part and a surface imaginary part.

Spectroscopic Strength Factors

The spectroscopic strength factor C^2S for the reaction $^{92}Zr(d,p)^{93}Zr$ is defined by the relation (private communication from P. D. Kunz)

$$\left(\frac{d\sigma}{d\Omega}\right)_{exp} = 1.53 \left(\frac{2J_f + 1}{2J_i + 1}\right) C^2S \frac{\left(\frac{d\sigma}{d\Omega}\right)_{DW}}{2J + 1} \tag{1}$$

where $(d\sigma/d\Omega)_{exp}$ and $(d\sigma/d\Omega)_{DW}$ are the experimental and DWBA calculated cross sections, respectively; C is the Clebsch-Gordan coefficient obtained by projecting the neutron isospin wave function onto that of the accepting nucleus and is 1 for a (d,p) reaction; and J, J_i, and J_f are the total angular momenta of the transferred particle, target nucleus, and residual nucleus, respectively. Also, for a particular J_f induced by a (d,p) reaction,

$$\sum_{\text{all } J_f\text{-levels}} \left(\frac{2J_f + 1}{2J_i + 1}\right) S$$

is defined as the number of holes in the J_f shell of the target nucleus, and $\sum_{\text{all } J_f\text{-levels}} S \leq 1$ is a measure of the fractional emptiness of that shell in the target nucleus. For an even-even target nucleus, such as $^{92}_{40}Zr_{52}$, expression (1) reduces to

$$\left(\frac{d\sigma}{d\Omega}\right)_{exp} = 1.53\, S \left(\frac{d\sigma}{d\Omega}\right)_{DW}$$

Similarly, for the reaction $^{92}Zr(d,t)^{91}Zr$, the spectroscopic strength factor C^2S is defined by the relation

$$\left(\frac{d\sigma}{d\Omega}\right)_{exp} = 3.33\, C^2S \frac{\left(\frac{d\sigma}{d\Omega}\right)_{DW}}{2J + 1} \qquad (2)$$

For a particular J_f induced by a (d,t) reaction,

$$\sum_{\text{all } J_f\text{-levels}} C^2S = \nu_{J_f} - \left(\frac{1}{N - Z + 1}\right) p_{J_f}$$

where

ν_{J_f} number of neutrons in the J_f shell in the target nucleus

N number of neutrons in the target nucleus

Z number of protons in the target nucleus

p_{J_f} number of protons in the J_f shell in the target nucleus

The sum is only over states of isospin $T_< = (N - Z)/2$ since states of isospin $T_> = (N - Z + 2)/2$ are too high to be observed in the present work.

RESULTS OF SINGLE-PARTICLE EXCITATION CALCULATIONS

Reaction $^{92}Zr(d, p)^{93}Zr$

In figure 4 are shown the measured angular distributions compared to the DWBA calculations which agree best with the data. In table IV are tabulated the excitation energies, momentum transfers, parities and possible spin assignments, and spectroscopic factors for 43 of the observed excited levels in ^{93}Zr which were made on the basis of DWBA calculations. The energy of the proton group resulting from the contaminant reaction $^{94}Zr(d, p_0)^{95}Zr$ interferes with that of a previously reported level at 0.260 MeV in ^{93}Zr (refs. 1 and 3). However, an upper limit of the spectroscopic strength factor for the reaction $^{92}Zr(d, p)^{93}Zr^{0.260}$ was determined by reducing the yield by the amount expected from the reaction $^{94}Zr(d, p_0)^{95}Zr$.

The levels populated in this stripping reaction were assumed to be those predicted by the shell model. Consequently, when the angular momentum transfer Δl had been determined, the correct shell model spin could be inferred with reasonable certainty since there is little ambiguity in this region of the periodic chart except for $\Delta l=2$ transitions. Since most of the expected strength of the $2d_{5/2}$ shell was found in the ground state, all other $\Delta l=2$ transitions with spectroscopic factors larger than 0.1 were expected to be $3/2^+$ states. This still left a number of $\Delta l=2$ states, however, for which assignments could not be made.

Assumed spin assignments based on shell model systematics and their respective spectroscopic strengths are tabulated in table V. In figure 6 are pictured the spectroscopic strengths of table V for each level belonging to a particular shell and the total strength of that shell drawn at the energy center of gravity of the several levels. For purposes of figure 6 and for center-of-gravity calculations, the $\Delta l=2$ states of unknown spin are included with the $d_{3/2}$ states. To an excitation energy of 4.84 MeV in ^{93}Zr, essentially all the expected strength was obtained for the $2d_{5/2}$, $3s_{1/2}$, $2d_{3/2}$, and $1g_{7/2}$ shells. The energy centroids of these shells were computed to lie at 0.00, 1.21, 2.23, and 2.37 MeV, respectively, in ^{93}Zr. In addition, there was found 43 percent of the $1h_{11/2}$ strength, 21 percent of the $2f_{7/2}$ strength, and 3 percent of the expected $3p_{3/2}$ strength. The energy centroids of these shells were calculated to lie above 2.31, 3.84, and 3.57 MeV, respectively, in ^{93}Zr.

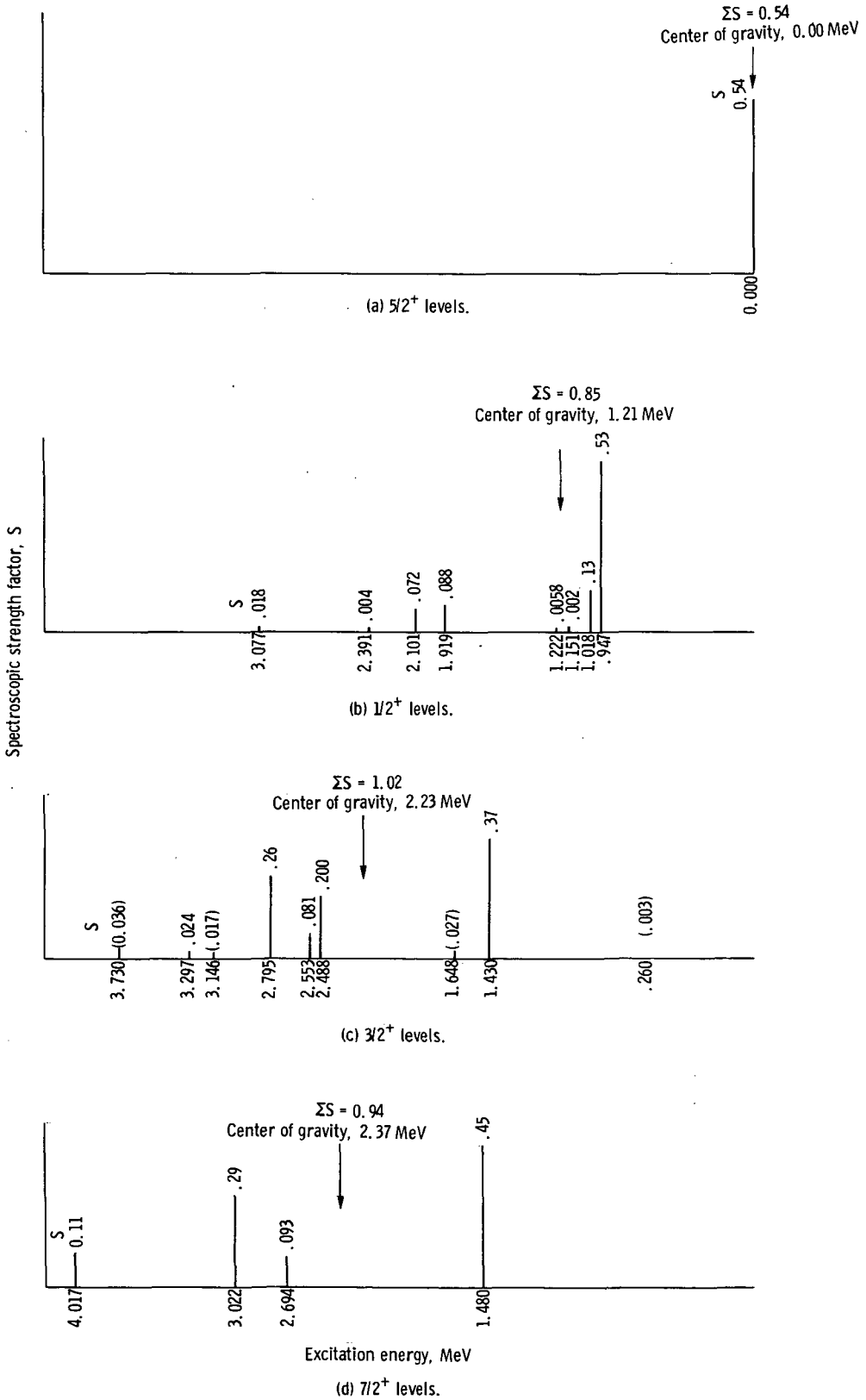

Figure 6. - Spectroscopic strength factors for levels excited in reaction $^{92}Zr(d, p)^{93}Zr$.

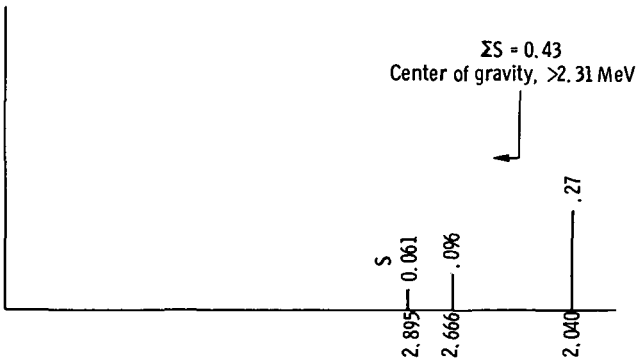

(e) 11/2⁻ levels.

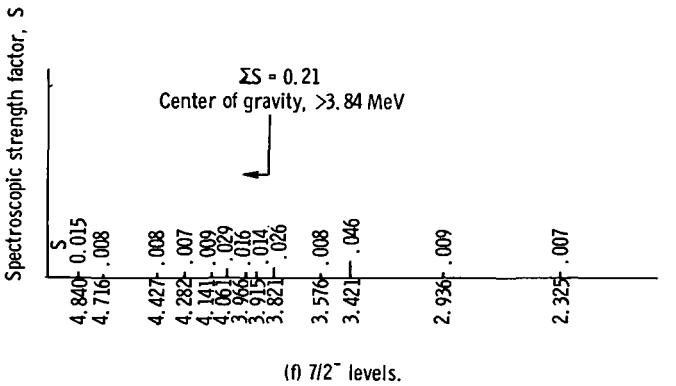

(f) 7/2⁻ levels.

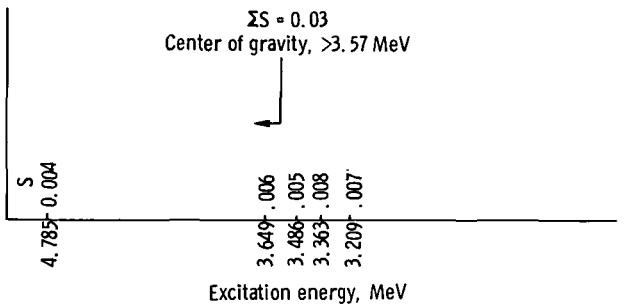

(g) 3/2⁻ levels.

Figure 6. - Concluded.

Reaction $^{92}Zr(d, t)^{91}Zr$

With the exception of the state at 1.196 MeV, the orbital momentum transfers for excitation of all other states were obtained by choosing the DWBA-calculated distributions which agree best with the data. In figure 5 are shown the calculated distributions compared to the data. Since no DWBA calculation was able to satisfactorily reproduce

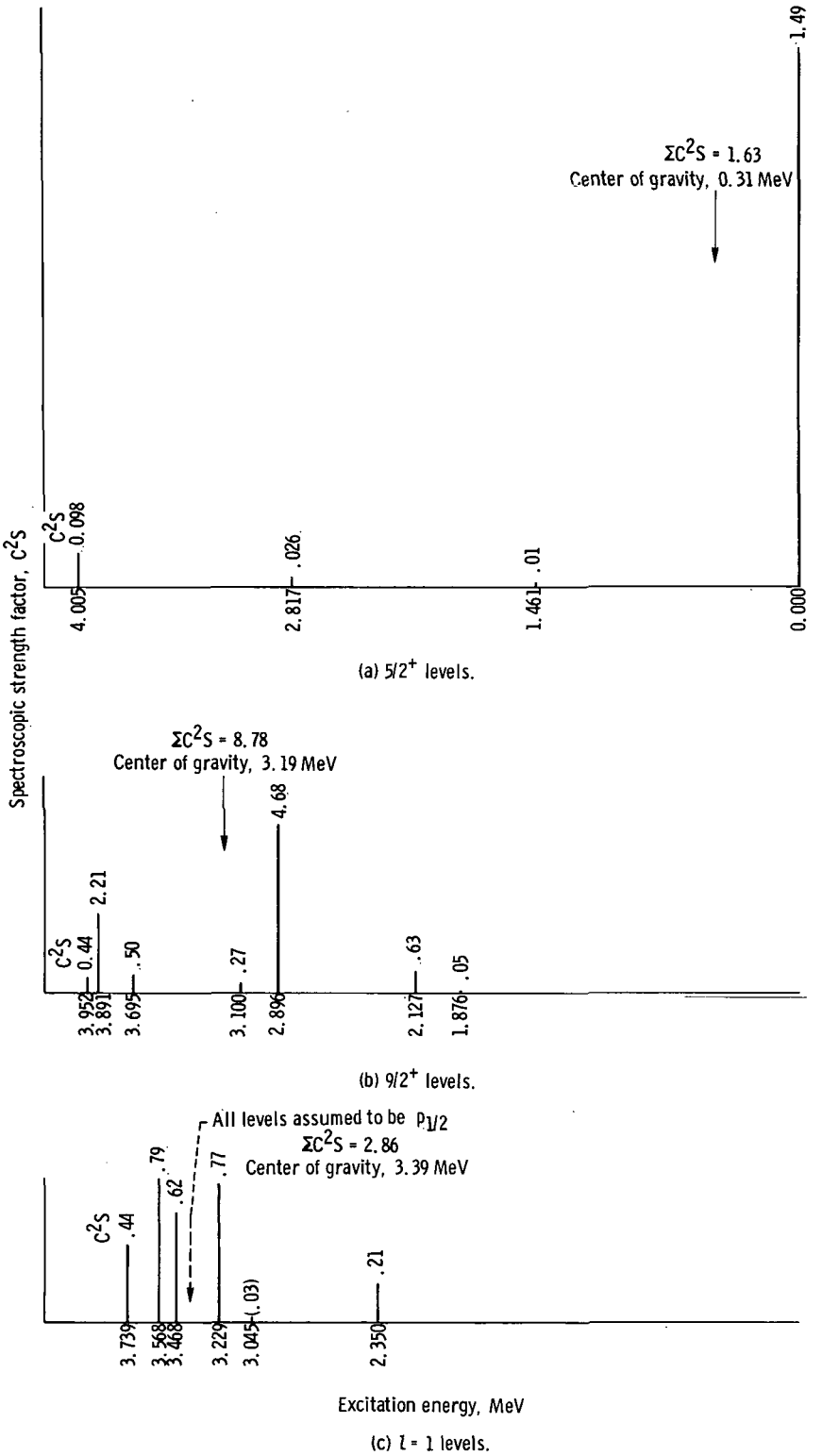

Figure 7. - Spectroscopic strength factors for levels excited in reaction $^{92}Zr(d,t)^{91}Zr$. (Not shown here are the 1.196-MeV ($1/2^+$), 2.036-MeV ($3/2^+$), 2.186-MeV ($7/2^+$), and 3.314-MeV ($1/2^+$) levels lying above the ^{92}Zr Fermi-sea.)

the data for the 1.196-MeV level, its orbital momentum transfer was assumed to be zero on the basis of previously reported spin assignments to this level (refs. 1, 4, 5, 7, 8, and 11). The $\Delta l=0$ DWBA calculation for this level is compared to the data in figure 5(d).

In table VI are tabulated the excitation energies, momentum transfers, parities and possible spin assignments, and spectroscopic strength factors for 21 of the observed excited ^{91}Zr levels which were made on the basis of the DWBA calculations. Several of the $\Delta l=2$ and $\Delta l=4$ transitions have been identified in other reaction studies (refs. 1, 4, and 5 to 11).

Assumed spin assignments based on shell model systematics and their respective spectroscopic strength factors are tabulated in table VII. All $\Delta l=2$ transitions were assumed to excite $5/2^+$ levels, except for the level of 2.036 MeV, which was previously reported to be $3/2^+$ (refs. 4, 5, 7, and 8). All $\Delta l=4$ transitions were assumed to excite $9/2^+$ levels, except for the level at 2.186 MeV, which was previously reported to be $7/2^+$ (refs. 5 and 7). In figure 7 are pictured the spectroscopic strengths listed in table VII for each level belonging to a particular shell and the total strength for that shell drawn at the energy center of gravity of the several levels. The summed strength of the several $5/2^+$ levels is 1.63, as compared to an expected summed strength of 2.0; and the energy center of gravity of the $5/2^+$ levels was computed to lie at 0.31 MeV. The summed strength of the assumed $9/2^+$ levels is 8.78 as compared to the expected value of 10, and their energy center of gravity was computed to lie at 3.19 MeV. Among the six $\Delta l=1$ transitions, the levels at 3.229, 3.468, and 3.568 MeV have also been previously observed in the (p,d) work (ref. 8) to be $\Delta l=1$ transitions. Most likely, most of the lower lying $\Delta l=1$ transitions are $1/2^-$ and will account for most of the expected strength of 1.85. However, it is expected that one or more of the higher lying levels represent neutrons picked up from the $2p_{3/2}$ shell. In addition, the summed strength of the two $1/2^+$ levels observed was 0.16, and their energy center of gravity was computed to lie at 1.99 MeV.

DISCUSSION

In both ^{91}Zr and ^{93}Zr, the single-particle neutron strengths appear to be very fragmented. In both nuclei this may be attributed to the presence of particle-core coupling configurations. This could result in the formation of a multiplet of levels for each pair of coupled core-spin and extra-core-nucleon-spin. For example, if J_{core} is the spin of the core state and j is the spin of the extra-core nucleon, then the possible number of observed levels in the multiplet is $2J_{core} + 1$ or $2j + 1$, whichever is smaller. In ^{93}Zr, for example, the odd neutron may be found in the $2d_{5/2}$, $3s_{1/2}$, $2d_{3/2}$, or $1g_{7/2}$ levels, while the core may exist in any of the possible states of ^{92}Zr. Considering only

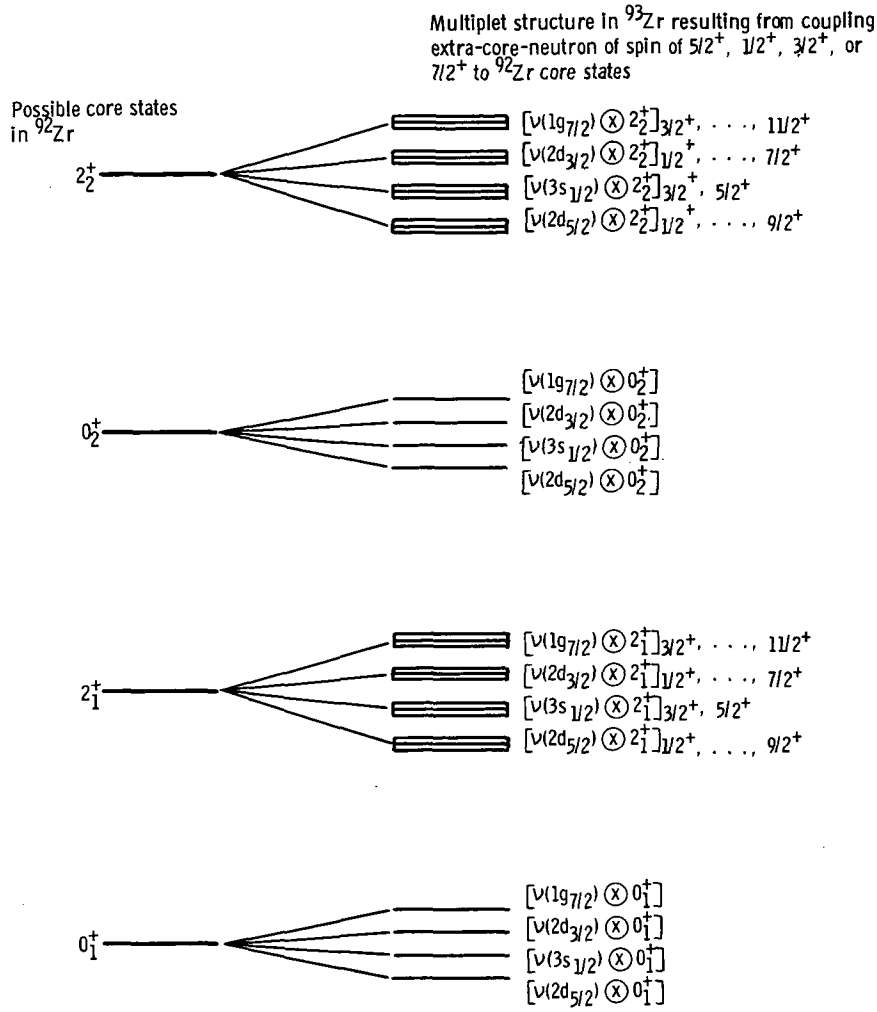

Figure 8. - Particle-core coupling construction.

the 0_1^+ (ground state), 2_1^+ (0.93 MeV), 0_2^+ (1.38 MeV), and 2_2^+ (1.83 MeV) states of ^{92}Zr, it is possible to construct six spin-1/2 states, 10 spin-3/2 states, 10 spin-5/2 states, and eight spin-7/2 states. These couplings are shown schematically in figure 8. The way in which such particle-core coupled states can be excited in a nuclear reaction depends on the nuclear structure model assumed.

Examples of models describing possibilities for excitation of excited-core states in a pickup and/or stripping reaction are as follows:

Example 1 - Assume that neither the target nor the residual nucleus contains any configuration mixing (i.e., extreme weak-coupling model) and that the ground state of the target nucleus, ^{92}Zr, can be written

$$\left[\nu\left(2d_{5/2}\right)_0^2 \otimes 0_1^+(^{90}Zr)\right]_{0_1^+(^{92}Zr)} \tag{3}$$

Then excited-core states cannot be populated via a direct reaction, but only through a second-order, two-step process. Such a process, illustrated in figure 9(a), might involve the addition or removal of a nucleon from the target nucleus followed by an inelastic scattering. This process could also take place in the reverse order, of course, as shown in figure 9(b).

Example 2 - If, in addition, one allows excited-core configurations in the ground state of the target nucleus, such as

$$\left[\nu\left(2d_{5/2}\right)_2^2 \otimes 2_1^+(^{90}Zr)\right]_{0_1^+(^{92}Zr)} \tag{4}$$

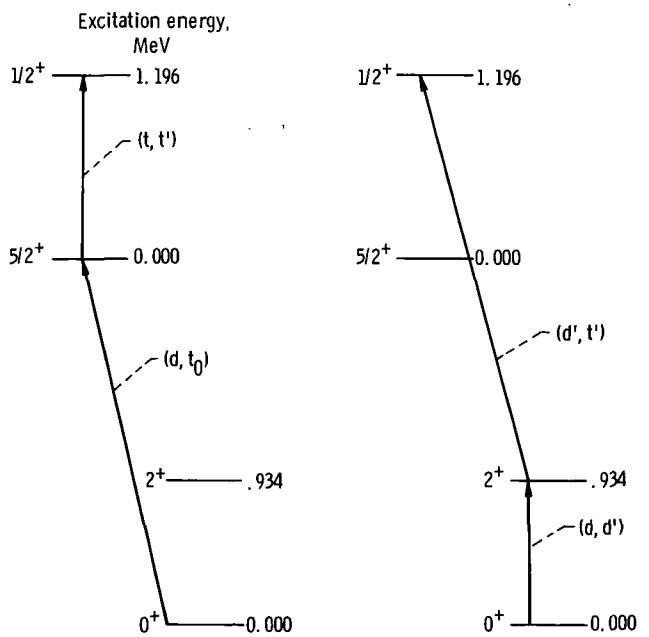

(a) Possible indirect process for reaction $^{92}Zr(d, t)^{91}Zr^{1.196}$

(b) Possible indirect process for reaction $^{92}Zr(d, t)^{91}Zr^{1.196}$

Figure 9. - Representation of possible indirect processes for reaction $^{92}Zr(d, t)^{91}Zr^{1.196}$

then excited-core states can be populated by a direct process, provided the spin of the final state is equal to that of the transferred nucleon. Otherwise, the excited-core states do not result from a direct reaction since the process involves a recoupling of the spins of the excited core and odd nucleon after the transfer reaction.

Example 3 - Still other excited-core states can be populated by a direct reaction if the residual nucleus is permitted to exhibit configuration mixing, a condition which is expected if the coupling between the core and the odd nucleon (or hole) is of finite strength. In the zirconium isotopes, the extensive splitting of single-particle strength indicates that this is the case. An excited-core state may then be reached via a direct reaction, provided it contains a component of the configuration

$$\left[\left(nl_{J_f}\right) \otimes 0_1^+(^{92}Zr)\right]_{J_f} \tag{5}$$

where the core $0_1^+(^{92}Zr)$ is the quantity described in equation (3) and $\left(nl_{J_f}\right)$ represents a hole or particle. The transition amplitude for population of such a state is proportional both to the amount of such an admixture in the final state and, as for all transfer reactions, to the fullness or emptiness of the $\left(nl_{J_f}\right)$ shell in the target nucleus. Of course, even with configuration mixing in the residual nucleus such states cannot be populated via direct pickup (stripping) reaction if the $\left(nl_{J_f}\right)$ shell of the target is empty (full). Thus, we see how excited-core states (i.e., states having a component of the configuration $\left[\nu(nl_j) \otimes J_{\text{excited core}}\right]_{J_f}$ as described in fig. 8) can be excited by a direct reaction as a consequence of configuration mixing. The total direct reaction strength given by equation (5) is divided among several J_f levels, some of which may be excited-core states.

Example 4 - As mentioned in example 3, the excitation of a state of spin J_f via a direct pickup (stripping) reaction can take place only if the target ground state is at least partially full (empty) a fraction of the time. As a consequence, for example, direct pickup reactions to particle states lying above the Fermi sea imply configuration mixing in the ground state of an even-even target, such as ^{92}Zr, of the form

$$\psi(^{92}\mathrm{Zr}) = a\left[\nu\left(2d_{5/2}\right)_0^2 \otimes 0_1^+(^{90}\mathrm{Zr})\right]_{0_1^+(^{92}\mathrm{Zr})} + b\left[\nu\left(3s_{1/2}\right)_0^2 \otimes 0_1^+(^{90}\mathrm{Zr})\right]_{0_1^+(^{92}\mathrm{Zr})}$$

$$+ c\left[\nu\left(2d_{3/2}\right)_0^2 \otimes 0_1^+(^{90}\mathrm{Zr})\right]_{0_1^+(^{92}\mathrm{Zr})} + d\left[\nu\left(1g_{7/2}\right)_0^2 \otimes 0_1^+(^{90}\mathrm{Zr})\right]_{0_1^+(^{92}\mathrm{Zr})} + \ldots \qquad (6)$$

The strengths of such transitions, provided they are known to be direct, then serve as a measure of the quantities a, b, c, d, etc. giving the size of a particular configuration in the target. In fact, the squares of these coefficients are the spectroscopic strength factors C^2S of equations (1) and (2).

The results of the experiments $^{90}\mathrm{Zr}(p,p')^{90}\mathrm{Zr}$ (refs. 9 to 11) and $^{90}\mathrm{Zr}(d,p)^{91}\mathrm{Zr}$ (refs. 4 and 5) have, in fact, been discussed from the point of view of the particle-core coupling reaction mechanism.

Reaction $^{92}\mathrm{Zr}(d,p)^{93}\mathrm{Zr}$

In table V are tabulated the excitation energies, momentum transfers, parities and assumed spin assignments, and spectroscopic strength factors for excited levels in $^{93}\mathrm{Zr}$ determined from the present work. The spins were assigned from shell model considerations. Also tabulated there for comparison are the results of previous (d,p) work by Cohen and Chubinsky (ref. 1) and Clarkson and Coker (ref. 3). However, the accuracy of both these previous works suffered experimental limitations more severe than those of the present work. Namely, the resolution of reference 1 is quoted to be 75 to 100 keV, compared to 35 to 45 keV in the present work; and the results of reference 3 were based on analyses of angular distributions for scattering angles larger than 50°, compared to 15° in the present work, and consequently might not be as reliable. Nevertheless, with a few exceptions, the agreement is seen to be rather good.

Also listed in table V are spins, parities, and spectroscopic strength factors for several levels of $^{93}\mathrm{Zr}$ determined from isobaric analog resonance (IAR) studies by means of the reaction $^{92}\mathrm{Zr}(p,p')$ (ref. 2). The l-values of the scattering resonances were determined from their interference patterns in the excitation curve. From this same experiment, spectroscopic strength factors were also obtained for these levels. Resonances were reported corresponding to the $^{93}\mathrm{Nb}$ isobaric analogs of nine $^{93}\mathrm{Zr}$ levels, all of which were observed in the present work. The assigned l-values agree with the present experiment in every case. Spins determined from the elastic IAR data

were assigned from shell model considerations. However, unique spins can be determined from the inelastic IAR data; and, in all comparable cases, the spin assignments of the present work based only on shell model systematics agree with the inelastic IAR determinations. Although the close-lying levels at 1.430 MeV($2d_{3/2}$) and 1.480 MeV ($1g_{7/2}$) were not resolved in reference 2, the inelastic IAR data confirmed the existence of the doublet at 2.488 and 2.553 MeV. Finally, the single-particle transfer spectroscopic factors determined from this (p,p) work agree rather well with those of the present work except for the states at 1.430 and 2.795 MeV.

Of the 10 states having $l=2$ observed in the present work, the ground state is known to have a spin of 5/2. Of the remaining nine $l=2$ states, five (E = 1.430, 2.488, 2.533, 2.795, and 3.297 MeV) have been found in the IAR work of reference 2 to contain excited core configurations and to have spins of 3/2. The other four $l=2$ states are sufficiently weak so that they could have spins of either 5/2 or 3/2 without affecting significantly the summed spectroscopic strengths. The state at 1.648 MeV was reported in references 1 and 3 to be $7/2^+$. However, the assignment in reference 1 is only tentative and that of reference 3 is based on scattering angles larger than 50°, which could lead to errors, particularly for weakly excited levels such as this one.

Eight states have been assigned $l=0$ and spin of 1/2 in the present work. Only one of these states is reported in reference 2 to have any significant amount of core excitation. This is the 1.919-MeV state, which was described as containing the configuration $\left[\nu(3s_{1/2}) \otimes 0_2^+\right]_{1/2^+}$ as well as some 2_3^+ strength coupled to an unknown particle state. The (d,p) work reported in references 1 and 3 is in agreement with the $l=0$ assignments for the states at 0.947 and 1.919 MeV; however, the $l=0$ state at 2.101 MeV reported in the present work was interpreted in reference 3 as an $l=4$ state. Since the experimental angular distribution of this $1/2^+$ level looks very much like the DWBA-calculated distribution for a $7/2^+$ level at scattering angles larger than 50°, the reason for the $7/2^+$ assignment in reference 3 is understandable. The remaining five states assigned $l=0$ herein were not observed in references 1 and 3. However, four of these are extremely weak, having spectroscopic strength factors of 0.02 or less in the present work.

Four levels are assigned $l=4$. One of these, at 3.022 MeV, also has been assigned a spin and parity of $7/2^+$ in the (d,p) work of references 1 and 3 and in the elastic IAR study of reference 2. Since it was not observed in any inelastic resonance, its core-excited components can be presumed to be small. None of the other three $l=4$ states observed herein were reported in previous works, even though the state at 1.480 MeV has a large spectroscopic strength factor of 0.45. This level is part of a doublet that was not resolved in reference 1.

Three $l=5$ states were observed in the present work and were assumed to have a spin of 11/2. Of these, two were observed in the (d,p) work of reference 3.

The $l=3$ strength is exceptionally fragmented, with 13 states observed up to an excitation energy of 4.840 MeV in ^{93}Zr. Assuming that all $l=3$ transitions are to $2f_{7/2}$ states accounts for only 21 percent of the expected $2f_{7/2}$ strength. Only the $l=3$ state at 3.421 MeV was seen in the (p,p') work (ref. 2), where it was found to contain a component $\left[\nu(2f_{7/2}) \otimes 0_2^+\right]_{7/2^-}$ as well as a component resulting from the coupling of the 3^- core state to an undetermined single-particle level. A weakly excited $l=3$ state at 2.325 MeV in the present work has been described previously as $l=4$ (refs. 1 and 3).

None of the five $l=1$ transitions has a ^{93}Nb analog which appeared as a resonance in the (p,p') work (ref. 2). All the $l=1$ states excited in the present work are quite weak, accounting for about 3 percent of the expected strength. Hence, it seems likely that a number of other $l=1$ states exist at higher energies.

Reaction $^{92}Zr(d,t)^{91}Zr$

In table VII are tabulated excitation energies, momentum transfers, parities and spin assignments which were assumed from shell model considerations, and spectroscopic strength factors for excited states in ^{91}Zr determined from the present work. Also tabulated there for comparison are the results of previous work leading to excited states of ^{91}Zr.

Inspection of figure 5 generally shows good agreement between the experimental and calculated angular distributions, with the exception of the three levels observed at 1.196 MeV ($1/2^+$), 2.036 MeV ($3/2^+$), and 2.186 MeV ($7/2^+$). The neutron pickup reactions for these excitations populate particle states lying above the ^{92}Zr Fermi-sea. This implies the likelihood that these excitations proceed in the manner described by examples 1 and/or 2 and/or 4 discussed earlier in this section; whereas all the other observed excitations can be considered to proceed in the manner described in example 3.

Among these three states, the most severe disagreement between the experimental distribution and the direct reaction calculation for single-particle excitations occurs for the 1.196-MeV level, as shown in figure 5(d). However, this level must be considered to be $1/2^+$ because of the many previously reported determinations of its spin and parity, as shown in table VII. The previously reported $^{92}Zr(d,t)^{91}Zr$ measurement (ref. 1) was made at only one angle, and a spin and parity assignment of $1/2^+$ for this level was inferred from the $1/2^+$ assignment given a level at about the same excitation energy from the reaction $^{90}Zr(d,p)^{91}Zr$ (ref. 1). Since then, the results of other experiments,

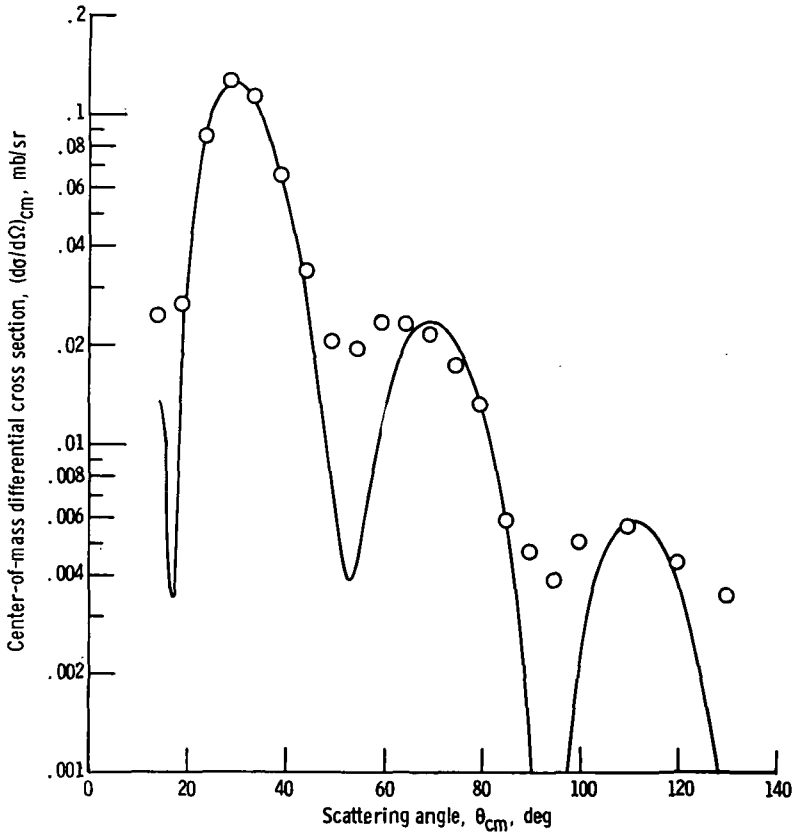

Figure 10. - Angular distribution of 1.196-MeV ($1/2^+$) level of ^{91}Zr excited by reaction $^{90}Zr(d,p)^{91}Zr_{1.196}$.

namely (d,p) (refs. 4 to 6), $(\alpha,n\gamma)$ (ref. 7), and (p,p') (refs. 9 to 11), have reported a $1/2^+$ level having an excitation energy of about 1.2 MeV in ^{91}Zr. Furthermore, pictured in figure 10 is the angular distribution of this level excited in the present work by the reaction $^{90}Zr(d,p)^{91}Zr$ due to the presence of ^{90}Zr contaminant in the target. It is shown compared to a DWBA-calculated angular distribution in which the level was assumed to be $1/2^+$. The agreement is seen to be very good and offers further confirmation of the $1/2^+$ nature of this level. Because of the overwhelming evidence for a $1/2^+$ level at about this excitation energy, it is reasonable to question the accuracy of the present (d,t) data. However, these data were taken at both the tandem facility of the Niels Bohr Institute and the tandem facility of the University of Pittsburgh, and the two sets of cross sections obtained are in excellent agreement. Very likely we are observing an indirect excitation here of the sort described in examples 1 and/or 2.

In addition, the $\Delta l=2$ calculated distribution for the level at 2.036 MeV is seen in figure 5(a) to differ significantly from the data at scattering angles greater than 40^o. However, the spin and parity of this level have been established to be $3/2^+$ by previous work (refs. 1, 4, 5, 7, and 8). Furthermore, from the results of the (d,p) work of reference 6 and the inelastic IAR scattering of reference 9, this level was interpreted

to have a large $\left[\nu(2d_{3/2}) \otimes 2_1^+\right]_{3/2^+}$ component. If this is truly the only $3/2^+$ level excited in this (d,t) reaction, the result of the single-particle excitation calculation implies an upper limit of approximately 10 percent probability of finding the neutron pair in the $2d_{3/2}$ orbital in the ^{92}Zr ground-state configuration as discussed in example 4. If this is an accurate description of the neutron pair, then the calculated distribution should show better agreement with the data. Instead, this $3/2^+$ level could be populated by the indirect processes described in examples 1 and/or 2 discussed at the beginning of this section. In such a case, it would be presumed to have a component $\left[\nu(2d_{5/2}) \otimes 2_1^+\right]_{3/2^+}$ and makes the 10-percent probability dubious.

Finally, although the $\Delta l=4$ calculated distribution for the weakly excited level at 2.186 MeV is seen in figure 5(b) to be in phase with the data, there is a significant difference in the peak-to-valley ratios. This level was previously reported (refs. 5 and 8) to be $7/2^+$. It is suggested in reference 5 that this level has either a component $\left[\nu(1g_{7/2}) \otimes 0_1^+\right]_{7/2^+}$ or one of the form $\left[\nu(2d_{5/2}) \otimes 2_1^+\right]_{7/2^+}$. The first of these two possibilities implies an admixture of $\left[\nu\left(1g_{7/2}\right)_0^2 \otimes 0_1^+\right]$ in the ground-state configuration of ^{92}Zr, as described in example 4. If this is the only $7/2^+$ level excited in the (d,t) reaction, the DWBA calculation implies an upper limit of approximately 13 percent probability of finding the neutron pair in the $1g_{7/2}$ orbital in the ^{92}Zr ground-state configuration. However, the second suggested configuration implies that this level is populated by indirect processes such as discussed in examples 1 and/or 2.

In addition to the ground state, several other $l=2$ levels in ^{91}Zr have been reported previously. The weakly excited 1.461-MeV level was previously reported (refs. 4, 5, 7, 9, and 11) to be $5/2^+$. It is suggested in references 5 and 9 that this level contains a predominant component of the form $\left[\nu(2d_{5/2}) \otimes 0_2^+\right]_{5/2^+}$. Another weakly excited level at 2.817 MeV was previously described as $5/2^+$ in reference 5, where it is suggested that this level consists primarily of a $\left[\nu(2d_{5/2}) \otimes 2_1^+\right]_{5/2^+}$ component.

Among the eight observed $l=4$ levels, five of them, including the previously mentioned 2.186-MeV level, have been reported previously. The weakly excited level at 1.876 MeV was described previously as either $9/2^+$ (refs. 5 and 11) or $7/2^+$ (refs. 4 and 7). In reference 11 it is suggested that this level is probably $9/2^+$, explained by $\left[\nu(2d_{5/2}) \otimes 2_1^+\right]_{9/2^+}$ coupling. The excited level at 2.127 MeV was previously de-

scribed as $9/2^+$ in references 7 and 8. The strongly excited level at 2.896 MeV was reported (refs. 7 and 8) previously to be $9/2^+$. In reference 8 it is suggested that it arises from a 2-particle - 1-hole excitation with one neutron hole in the $1g_{9/2}$ level and a pair of zero coupled neutrons in the $2d_{5/2}$ level; that is, $\left[\nu\left(2d_{5/2}\right)_0^2 \otimes \nu\left(1g_{9/2}\right)^{-1}\right]_{9/2^+}$, or equivalently $\left[\nu\left(1g_{9/2}\right)^{-1} \otimes 0_1^+\right]_{9/2^+}$, where the core state, when coupled to a hole, refers to the target nucleus. The weakly excited level at 3.695 MeV was reported in reference 8 to be $9/2^+$, and it is suggested there that this level arises from the coupling of a $1g_{9/2}$ hole with a 2^+ state of a neutron pair, that is, $\left[\nu\left(2d_{5/2}\right)_{2^+}^2 \otimes \nu\left(1g_{9/2}\right)^{-1}\right]_{9/2^+}$. However, this state could equally likely have a component $\left[\nu\left(1g_{9/2}\right)^{-1} \otimes 2_1^+\right]_{9/2^+}$. Similarly, the rather strongly excited level at 3.891 MeV could result from the coupling $\left[\nu\left(1g_{9/2}\right)^{-1} \otimes 0_2^+\right]_{9/2^+}$.

Four of the six observed $\Delta l=1$ transitions were reported previously. The weakly excited level at 2.350 MeV was reported in reference 7 to be $1/2^-$. It results most probably from the pickup of a $2p_{1/2}$ neutron from the core, resulting in a coupling of $\left[\nu\left(2p_{1/2}\right)^{-1} \otimes 0_2^+\right]_{1/2^-}$ or $\left[\nu\left(2p_{1/2}\right)^{-1} \otimes 0_1^+\right]_{1/2^-}$. The levels at 3.229, 3.468, and 3.568 MeV were reported in reference 8 to be either $1/2^-$ or $3/2^-$. However, the level at 3.739 MeV was reported therein to be $l=2$, in contradiction to the result of the present work where it is well described as an $l=1$ transition resulting in a spin and parity assignment of either $1/2^-$ or $3/2^-$.

The weakly excited $1/2^+$ level at 3.314 MeV could well be the same $1/2^+$ level reported in reference 5 at 3.332 MeV.

CONCLUSIONS

Reaction $^{92}Zr(d, p)^{93}Zr$

The experimental angular distributions measured in the reaction $^{92}Zr(d,p)^{93}Zr$ agree well in all cases with DWBA direct single-particle reaction calculations. However, the fragmentation of the expected single-particle strengths suggests that many levels result from particle-core coupling processes. From the results of the previous isobaric analog resonance work of Kent, Lieb, and Moore and the (d,p) spectroscopic strength factors measured herein, we can conclude that the ^{93}Zr levels at 0.000 MeV ($5/2^+$), 0.947 MeV ($1/2^+$), 1.430 MeV ($3/2^+$), 2.488 MeV ($3/2^+$), 2.795 MeV ($3/2^+$), 1.480 MeV ($7/2^+$), 3.022 MeV ($7/2^+$), and 2.040 MeV ($11/2^-$) have the largest amount of single-particle strength in their respective shells. Many of the core-excited components of the $3/2^+$ levels already have been measured explicitly. However, it can be expected that future IAR work will reveal many more core-excited components for all of the levels of ^{93}Zr. Furthermore, most of the expected single-particle strength of the $2d_{5/2}$, $3s_{1/2}$, $2d_{3/2}$, and $1g_{7/2}$ shells was observed, as well as partial single-particle population of the $1h_{11/2}$, $2f_{7/2}$, and $3p_{3/2}$ shells.

Reaction $^{92}Zr(d, t)^{91}Zr$

The good agreement of DWBA direct single-particle reaction calculations with the (d,p) data was not obtained for several of the ^{91}Zr levels that were excited in the (d,t) reaction. In particular, these were the 1.196-MeV ($1/2^+$), 2.036-MeV ($3/2^+$), and 2.186-MeV ($7/2^+$) levels which lie above the ^{92}Zr Fermi-sea. Consequently, it is quite likely that the (d,t) reaction for excitation of these levels proceeds to a particle-core coupled state either by an indirect process, or else by a direct process made possible by configuration mixing in the ^{92}Zr ground state.

Among these three levels, the disagreement is most notable for the $1/2^+$ level of ^{91}Zr at 1.196 MeV, despite the fact that the measured angular distribution of this level excited by the reaction $^{90}Zr(d,p)^{91}Zr^{1.196}$ agrees so well with the results of the direct single-particle reaction calculation. This is reasonable when one considers that the (d,p) reaction proceeds from a target nucleus, ^{90}Zr, whose $3s_{1/2}$ shell is empty and which can have only very small collective core components due to its closed-shell nature. Consequently, there is only very small overlap with any possible collective component in the 1.196-MeV level of ^{91}Zr. However, the (d,t) reaction to this level can proceed if the ^{92}Zr ground-state configuration

(1) Has a component $\left[\nu\left(3s_{1/2}\right)^2_{0^+}\right]$, which would result in a direct single-particle excitation

(2) And/or is represented as $\left[\nu\left(2d_{5/2}\right)^2_{0^+} \otimes 0^+_1\right]$ and undergoes pickup to the ground state of ^{91}Zr and subsequent inelastic excitation to the 1.196-MeV level having a component $\left[\nu(2d_{5/2}) \otimes 2^+_1\right]_{1/2^+}$ (this indirect process can proceed in the reverse order also)

(3) And/or has some collective ground-state configuration such as $\left[\nu\left(2d_{5/2}\right)^2_{2^+} \otimes 2^+_1\right]_{0^+}$, which makes possible an indirect (d,t) process leading to the 1.196-MeV level having a component $\left[\nu(2d_{5/2}) \otimes 2^+_1\right]_{1/2^+}$

Should the reaction proceed by some such collective mechanism, it is not clear what the angular distribution would be. In fact, a recent calculation by Paradellis, Hontzeas, and Blok[1] of the structure of some zirconium isotopes assuming the unified nuclear model indicates that the ^{92}Zr ground-state configuration is about 90-percent $\left[\nu\left(2d_{5/2}\right)^2_{0^+}\right]$ and about 10-percent $\left[\nu\left(2d_{5/2}\right)^2_{2^+} \otimes 2^+_1\right]_{0^+}$. Furthermore, the configuration of the 1.196-MeV ($1/2^+$) level of ^{91}Zr is indicated therein to be about 65-percent $\left[\nu(3s_{1/2})\right]$ with a collective component of about 32-percent $\left[\nu(2d_{5/2}) \otimes 2^+_1\right]_{1/2^+}$, that is, a $5/2^+$ neutron coupled to a one-phonon quadrupole collective core excitation. Thus, it is quite possible that the reaction ^{92}Zr(d,t)^{91}Zr$^{1.196}$ is a complicated process involving perhaps some collective core excitation. Consequently, it is not too surprising that a direct reaction calculation for single-particle excitation disagrees with the measured angular distribution of the 1.196-MeV level of ^{91}Zr excited in the (d,t) pickup reaction. Furthermore, one might expect that the direct reaction calculation for the reaction ^{92}Zr(p,d)^{91}Zr$^{1.196}$ measured by Ball and Fulmer would, as for the (d,t) reaction, disagree with the measured angular distribution. However, it would not be too surprising if this were not so, because of the relatively complicated possibilities for exciting states lying above the Fermi-sea in neutron pickup reactions. The measured

[1]Nuclear Physics, Vol. A168, 1971, pp. 539-560.

distributions could well depend on the nature of the incident particle and its energy in a way that is unrelated to the direct reaction theory for single-particle excitations used in these calculations.

From the (d,t) spectroscopic strength factors measured here, it can be concluded that the 0.000 MeV ($5/2^+$), 2.896 MeV ($9/2^+$), 3.891 MeV ($9/2^+$), 3.229 MeV ($1/2^-$, $3/2^-$), 3.468 MeV ($1/2^-, 3/2^-$), 3.568 MeV ($1/2^-, 3/2^-$), and 3.739 MeV ($1/2^-, 3/2^-$) have the largest amount of single-hole strength in their respective shells. Furthermore, most of the expected strength of the $2d_{5/2}$, $1g_{9/2}$, and (very likely) $2p_{1/2}$ shells was observed, as well as partial population of the $2p_{3/2}$, $3s_{1/2}$, $2d_{3/2}$, and $1g_{7/2}$ shells.

CONCLUDING REMARKS

The observed departure of the level structure of ^{91}Zr and ^{93}Zr from what one would expect in a single-particle model is to be expected from previous (p,p') work (refs. 2 and 9 to 11), where attempts were made to explain the level structure of these nuclei as resulting from particle-core coupling. Many of the levels of ^{91}Zr reported in the present work are presumed in references 5, 9, 10, and 11 to arise from such coupling schemes. Consequently, it should be no surprise that such significant fragmentation of the single-particle strength can be observed in the structure of ^{91}Zr and ^{93}Zr.

From the spectroscopic strengths measured in the (d,t) reaction, it can be concluded that the ^{92}Zr ground-state configuration is at least 71-percent $\left(2d_{5/2}\right)^2_{0^+}$ and has an upper limit of 7-percent $\left(3s_{1/2}\right)^2_{0^+}$, 9-percent $\left(2d_{3/2}\right)^2_{0^+}$, and 13-percent $\left(1g_{7/2}\right)^2_{0^+}$ This agrees reasonably well with the conclusion for the ^{92}Zr ground-state configuration reported in references 1 and 8.

Lewis Research Center,
National Aeronautics and Space Administration,
Cleveland, Ohio, May 10, 1972,
112-02.

REFERENCES

1. Cohen, Bernard L.; and Chubinsky, Oleg V.: Nuclear Structure Studies in the Zirconium Isotopes with (d,p) and (d,t) Reactions. Phys. Rev., vol. 131, no. 5, Sept. 1, 1963, pp. 2184-2192.

2. Kent, James J.; Lieb, K. P.; and Moore, C. Fred: Isobaric Analog Resonances in ^{92}Zr (p,p'). Phys. Rev., vol. C1, no. 1, Jan. 1970, pp. 336-345.

3. Clarkson, R. G.; and Coker, W. R.: Charge Exchange in ^{92}Zr(d,p)^{93}Zr. Phys. Rev., vol. C2, no. 3, Sept. 1970, pp. 1108-1115.

4. Bingham, C. R.; and Halbert, M. L.: Neutron Shell Structure in ^{91}Zr and ^{92}Zr by (d,p) and (α,^{3}He) Reactions. Phys. Rev., vol. C2, no. 6, Dec. 1970, pp. 2297-2309.

5. Graue, A.; Herland, L. H.; Lervik, K. J.; Neese, J. T.; and Cosman, E. R.: The ^{90}Zr(d,p)^{91}Zr Reaction with High Resolution. Nucl. Phys., vol. A187, no. 1, May 29, 1972, pp. 141-152.

6. Clarkson, R. G.; Coker, W. R.; and Moore, C. F.: Effects of Charge Exchange in ^{90,91}Zr(d,p). Phys. Rev., vol. C2, no. 3, Sept. 1970, pp. 1097-1108.

7. Glenn, J. E.; Baer, H. W.; and Kraushaar, J. J.: Spectroscopy of States in ^{91}Zr from p-Ray Transitions Observed in the ^{88}Sr(α,np)^{91}Zr Reaction. Nucl. Phys., vol. A165, no. 3, Apr. 19, 1971, pp. 533-544.

8. Ball, J. B.; and Fulmer, C. B.: Neutron Hole States in Z=40 Nuclei Studied with the (p,d) Reaction on ^{90}Zr, ^{91}Zr, and ^{92}Zr. Phys. Rev., vol. 172, no. 4, Aug. 20, 1968, pp. 1199-1207.

9. Moore, C. Fred; Zaidi, S. A. A.; and Kent. J. J.: Single-Particle States Built on the Second 0^{+} State in ^{90}Zr. Phys. Rev. Letters, vol. 18, no. 10, Mar. 6, 1967, pp. 345-346.

10. Lieb, K. P.; Kent, James J.; and Moore, C. Fred: Isobaric-Analog Study of ^{90}Zr. Phys. Rev., vol. 175, no. 4, Nov. 20, 1968, pp. 1482-1493.

11. DuBard, James L.; and Sheline, Raymond K.: High-Resolution Proton Scattering on Zr^{91} and the Core-Excitation Model. Phys. Rev., vol. 182, no. 4, June 20, 1969, pp. 1320-1328.

12. Kern, Jean: Computer Analysis of Nuclear Spectra and p-Energy Standards. Nucl. Inst. Methods, vol. 79, 1970, pp. 233-239.

13. Becchetti, F. D., Jr.; and Greenlees, G. W.: Nucleon-Nucleus Optical-Model Parameters, $A > 40$, $E < 50$ MeV. Phys. Rev., vol. 182, no. 4, June 20, 1969, pp. 1190-1209.

14. Becchetti, F. D., Jr.; and Greenlees, G. W.: General Set of ^{3}He and Triton Optical-Model Potentials for $A > 40$, $E < 40$ MeV. Proceedings of the Third International Symposium on Polarization Phenomena in Nuclear Reactions. H. H. Barschall and W. Haeberli, eds., University of Wisconsin Press, 1971, pp. 682-683.

15. Smith, Margaret M.; and Giamati, Charles C.: Expanded Fortran IV Program for Elastic Scattering Analyses. NASA TN D-6000, 1970.

16. Paradellis, Th.; Hontzeas, S.; and Blok, H.: Unified-Model Calculations in Some Zr Isotopes. Nucl. Phys., vol. A168, 1971, pp. 539-560.

TABLE I. - DIFFERENTIAL CROSS SECTIONS FOR LEVELS INDUCED BY REACTION $^{92}Zr(d,p)^{93}Zr$

Center-of-mass scattering angle, θ_{cm}, deg	Differential cross section, $\frac{d\sigma}{d\Omega}$, mb/sr	Statistical error of differential cross section, $\pm\Delta\frac{d\sigma}{d\Omega}$, mb/sr	Center-of-mass scattering angle, θ_{cm}, deg	Differential cross section, $\frac{d\sigma}{d\Omega}$, mb/sr	Statistical error of differential cross section, $\pm\Delta\frac{d\sigma}{d\Omega}$, mb/sr
$^{92}Zr(d,p)^{93}Zr^{g.s.}$			$^{92}Zr(d,p)^{93}Zr^{0.947}$		
15.20	6.14	1.81×10^{-1}	15.20	2.06	7.41×10^{-2}
20.27	7.27	1.57	20.27	1.52	4.83
25.33	6.44	1.44	25.33	4.04	9.87
30.39	3.78	3.69×10^{-2}	30.39	5.76	5.17
35.45	2.04	2.96	35.45	4.93	6.03
40.51	1.78	2.30	40.51	3.16	3.55
45.56	2.43	1.82	45.56	1.75	1.54
50.60	2.66	2.45	50.60	1.10	1.26
55.65	2.47	2.88	55.65	1.01	1.44
60.68	1.80	2.41	60.68	1.15	1.71
65.71	9.98×10^{-1}	1.57	65.71	1.08	1.67
70.74	5.90	8.99×10^{-3}	70.74	9.58×10^{-1}	1.31
75.76	5.58	1.03×10^{-2}	75.76	8.18	1.38
80.78	5.62	9.59×10^{-3}	80.78	5.73	9.66×10^{-3}
85.78	6.82	1.06×10^{-2}	85.78	3.92	7.01
90.79	6.01	6.09×10^{-3}	90.79	2.35	3.81
95.78	4.55	8.92	95.78	1.80	4.37
100.78	3.17	8.63	100.78	1.78	5.43
110.74	1.71	4.35	110.74	2.06	4.77
120.68	1.40	5.69	120.68	1.64	6.35
130.60	1.62	7.00	130.60	9.90×10^{-2}	4.83
140.57	1.58	4.59	140.57	7.15	3.09
$^{92}Zr(d,p)^{93}Zr^{0.260}$ (a)			$^{92}Zr(d,p)^{93}Zr^{1.018}$		
15.20	1.95×10^{-2}	1.11×10^{-2}	15.20	9.14×10^{-2}	1.73×10^{-2}
20.27	2.65	1.13	20.27	8.43	1.03
25.33	2.17	1.04	25.33	9.50	1.14
30.39	1.36	3.44×10^{-3}	35.45	1.19×10^{-1}	6.54×10^{-3}
35.45	9.53×10^{-3}	3.07	40.51	7.13×10^{-2}	4.23
40.51	8.48	2.61	45.56	4.28	2.41
45.56	9.45	2.30	50.60	2.94	2.20
50.60	9.70	2.04	55.65	2.47	2.34
55.65	7.90	2.12	60.68	2.52	2.89
60.68	5.37	1.76	65.71	2.15	2.10
65.71	3.18	1.36	70.74	2.55	1.88
70.74	2.28	8.72×10^{-4}	75.76	2.27	2.20
75.76	3.28	1.24×10^{-3}	80.78	1.41	1.66
80.78	3.13	9.99×10^{-4}	85.78	8.49×10^{-3}	1.55
85.78	3.65	1.08×10^{-3}	90.79	5.06	6.17×10^{-4}
90.79	2.40	7.81×10^{-4}	95.78	4.08	7.68
95.78	2.20	7.68	100.78	5.99	9.59
100.78	1.34	7.19	110.74	4.21	6.82
110.74	5.37×10^{-4}	4.95	120.68	3.07	7.66
120.68	6.12	5.47			
130.60	7.92	7.25			
140.57	5.83	5.65			

[a]Cross sections $d\sigma/d\Omega$ are reduced by yield from contaminant reaction $^{94}Zr(d,p_0)^{95}Zr$.

TABLE I. - Continued. DIFFERENTIAL CROSS SECTIONS FOR LEVELS INDUCED BY REACTION $^{92}Zr(d,p)^{93}Zr$

Center-of-mass scattering angle, θ_{cm}, deg	Differential cross section, $\frac{d\sigma}{d\Omega}$, mb/sr	Statistical error of differential cross section, $\pm\Delta\frac{d\sigma}{d\Omega}$, mb/sr	Center-of-mass scattering angle, θ_{cm}, deg	Differential cross section, $\frac{d\sigma}{d\Omega}$, mb/sr	Statistical error of differential cross section, $\pm\Delta\frac{d\sigma}{d\Omega}$, mb/sr
$^{92}Zr(d,p)^{93}Zr^{1.151}$			$^{92}Zr(d,p)^{93}Zr^{1.430}$		
15.20	1.54×10^{-2}	6.67×10^{-3}	15.20	2.86	9.63×10^{-2}
25.33	1.66	5.40	20.27	3.35	8.54
30.39	2.03	2.58	25.33	2.94	7.89
35.45	1.37	2.45	30.39	1.78	2.32
40.51	1.25	1.95	35.45	1.07	2.02
45.56	2.17×10^{-3}	9.49×10^{-4}	40.51	9.81×10^{-1}	1.69
50.60	1.88	1.14×10^{-3}	45.56	1.18	1.26
55.65	4.34	1.34	50.60	1.15	1.41
60.68	1.21	1.02	55.65	1.02	1.57
65.71	3.77	9.96×10^{-4}	60.68	6.91×10^{-1}	1.37
70.74	3.22	8.05	65.71	4.24	9.65×10^{-3}
75.76	2.67	9.55	70.74	3.07	6.64
85.78	1.62	6.74	75.76	3.28	8.02
90.79	4.32×10^{-4}	3.70	80.78	3.10	6.93
95.78	1.06×10^{-3}	4.73	85.78	3.39	7.07
100.78	4.80×10^{-4}	5.59	90.79	2.73	4.11
			95.78	2.00	5.32
			100.78	1.36	5.12
			110.74	8.69×10^{-2}	3.10
			120.68	9.21	5.04
			130.60	1.00×10^{-1}	5.55
			140.57	9.50×10^{-2}	3.56
$^{92}Zr(d,p)^{93}Zr^{1.222}$			$^{92}Zr(d,p)^{93}Zr^{1.480}$		
15.20	2.22×10^{-2}	7.41×10^{-3}	15.20	4.74×10^{-1}	3.70×10^{-2}
20.27	1.95	6.17	20.27	4.96	3.50
25.33	5.14	8.31	25.33	5.71	3.43
30.39	6.39	3.95	30.39	6.21	1.48
35.45	5.60	3.88	35.45	5.77	1.51
40.51	3.70	2.93	40.51	5.85	1.34
45.56	1.79	1.56	45.56	4.87	8.13×10^{-3}
50.60	1.04	1.47	50.60	3.73	9.05
55.65	9.36×10^{-3}	1.56	55.65	2.80	9.47
60.68	1.26×10^{-2}	1.63	60.68	2.72	9.92
65.71	1.02	1.36	65.71	2.36	7.76
70.74	8.65×10^{-3}	1.07	70.74	2.16	5.77
75.76	8.98	1.24	75.76	2.11	6.59
80.78	5.06	8.66×10^{-4}	80.78	1.56	5.33
85.78	2.76	7.41	85.78	1.27	4.99
90.79	1.60	4.32	90.79	8.87×10^{-2}	2.34
95.78	2.95×10^{-4}	4.14	95.78	7.43	3.66
100.78	1.36×10^{-3}	5.59	100.78	6.79	3.84
110.74	2.21	4.95	110.74	7.68	2.92
120.68	2.96	6.57	120.68	6.61	4.38
130.60	7.25×10^{-4}	4.83	130.60	3.90	3.98
			140.57	2.57	1.85

TABLE I. - Continued. DIFFERENTIAL CROSS SECTIONS FOR LEVELS INDUCED BY REACTION $^{92}Zr(d,p)^{93}Zr$

Center-of-mass scattering angle, θ_{cm}, deg	Differential cross section, $\frac{d\sigma}{d\Omega}$, mb/sr	Statistical error of differential cross section, $\pm\Delta\frac{d\sigma}{d\Omega}$, mb/sr	Center-of-mass scattering angle, θ_{cm}, deg	Differential cross section, $\frac{d\sigma}{d\Omega}$, mb/sr	Statistical error of differential cross section, $\pm\Delta\frac{d\sigma}{d\Omega}$, mb/sr
$^{92}Zr(d,p)^{93}Zr^{1.648}$			$^{92}Zr(d,p)^{93}Zr^{2.040}$		
15.20	1.74×10^{-1}	1.73×10^{-2}	25.34	2.71×10^{-1}	2.07×10^{-2}
20.27	2.39	1.75	30.40	3.23	9.43×10^{-3}
25.33	2.11	1.66	35.46	3.60	9.58
30.39	1.55	6.18×10^{-3}	40.52	4.27	9.60
35.45	1.06	5.72	45.57	4.32	1.02×10^{-2}
40.51	8.00×10^{-2}	4.56	50.62	3.79	7.66×10^{-3}
45.56	8.28	3.35	55.66	3.41	8.57
50.60	8.28	3.26	60.70	3.14	9.28
55.65	7.18	3.56	65.73	2.57	7.12
60.68	5.94	3.51	70.76	2.45	5.90
65.71	3.75	2.73	75.78	2.72	7.55
70.74	2.83	2.08	80.79	2.33	5.99
75.76	3.19	2.29	85.80	2.27	4.99
80.78	2.30	1.93	90.81	1.69	4.14
85.78	2.67	1.89	95.80	1.15	3.25
90.79	1.93	1.09	100.79	8.72×10^{-2}	2.64
95.78	1.51	1.30			
100.78	1.52	1.68			
110.74	7.31×10^{-3}	8.99×10^{-4}			
120.68	1.03×10^{-2}	1.31×10^{-3}			
130.60	6.52×10^{-3}	1.45			
140.57	1.12×10^{-2}	3.34			
$^{92}Zr(d,p)^{93}Zr^{1.919}$			$^{92}Zr(d,p)^{93}Zr^{2.101}$		
20.28	4.71×10^{-1}	2.57×10^{-2}	15.21	6.02×10^{-1}	2.72×10^{-2}
25.34	7.79	3.53	20.28	6.21	4.82
30.40	1.01	1.78	25.34	7.63	3.73
35.46	9.13×10^{-1}	1.57	30.40	7.69	1.51
40.52	6.60	1.19	35.46	7.04	1.37
45.57	4.35	9.61×10^{-3}	40.52	5.42	1.09
50.62	2.78	5.86	45.57	4.08	9.88×10^{-3}
55.66	2.29	6.23	50.62	2.95	6.84
60.70	2.37	7.15	55.66	2.66	7.45
65.73	2.13	5.97	60.70	2.40	8.28
70.76	1.96	4.83	65.73	1.83	6.07
75.78	1.79	5.44	70.76	1.56	4.56
80.79	1.39	3.99	75.78	1.44	5.25
85.80	1.11	3.03	80.79	1.13	3.93
90.81	7.76×10^{-2}	2.41	85.80	1.03	3.50
95.80	5.29	1.95	90.81	7.56×10^{-2}	2.90
100.79	4.69	1.94	95.80	5.37	2.31
			100.79	4.28	1.85

TABLE I. - Continued. DIFFERENTIAL CROSS SECTIONS FOR LEVELS INDUCED BY REACTION $^{92}Zr(d,p)^{93}Zr$

Center-of-mass scattering angle, θ_{cm}, deg	Differential cross section, $\frac{d\sigma}{d\Omega}$, mb/sr	Statistical error of differential cross section, $\pm\Delta\frac{d\sigma}{d\Omega}$, mb/sr	Center-of-mass scattering angle, θ_{cm}, deg	Differential cross section, $\frac{d\sigma}{d\Omega}$, mb/sr	Statistical error of differential cross section, $\pm\Delta\frac{d\sigma}{d\Omega}$, mb/sr
$^{92}Zr(d,p)^{93}Zr$ 2.325			$^{92}Zr(d,p)^{93}Zr$ 2.488		
20.28	1.02×10^{-1}	1.33×10^{-2}	15.21	1.75	4.64×10^{-2}
25.34	8.51×10^{-2}	1.35	20.28	2.17	7.18
30.40	1.09×10^{-1}	6.34×10^{-3}	25.34	1.78	6.22
35.46	6.87×10^{-2}	5.10	30.40	1.15	2.02
40.52	5.82	4.39	35.46	7.71×10^{-1}	1.47
45.57	4.41	3.66	40.52	7.86	1.38
50.62	3.05	2.93	45.57	7.86	1.49
55.66	4.55	3.56	50.62	7.53	1.19
60.70	5.02	4.26	55.66	6.78	1.37
65.73	2.67	3.46	60.70	5.70	1.32
70.76	2.12	2.01	65.73	3.30	8.27×10^{-3}
75.78	9.74×10^{-3}	3.06	70.76	2.35	5.63
80.79	1.05×10^{-2}	1.60	75.78	2.14	6.30
85.80	1.37	1.75	80.79	2.01	5.39
90.81	1.58	1.54	85.80	2.30	4.99
95.80	1.51	1.36	90.81	2.08	4.69
100.79	9.11×10^{-3}	9.59×10^{-4}	95.80	1.55	3.90
			100.79	1.21	3.11
$^{92}Zr(d,p)^{93}Zr$ 2.391			$^{92}Zr(d,p)^{93}Zr$ 2.553		
40.52	9.11×10^{-3}	2.77×10^{-3}	15.21	8.42×10^{-1}	3.22×10^{-2}
50.62	4.15	2.36	20.28	9.07	4.21
55.66	6.23	2.45	25.34	7.21	3.53
65.73	8.80	2.09	30.40	5.22	1.25
70.76	1.06×10^{-2}	1.68	35.46	3.24	9.58×10^{-3}
75.78	5.06×10^{-3}	1.72	40.52	4.22	1.01×10^{-2}
80.79	4.32	1.53	45.57	2.92	8.53×10^{-3}
85.80	4.04	1.28	50.62	3.00	7.17
90.81	3.27	1.05	55.66	2.84	7.90
95.80	1.72	8.28×10^{-4}	60.70	2.38	8.03
100.79	8.79×10^{-4}	6.39	65.73	1.45	5.24
			70.76	1.00	3.55
			75.78	8.69×10^{-2}	4.01
			80.79	7.52	3.19
			85.80	8.98	3.23
			90.81	7.18	2.84
			95.80	5.78	2.37
			100.79	4.09	1.81

TABLE I. - Continued. DIFFERENTIAL CROSS SECTIONS FOR LEVELS INDUCED BY REACTION $^{92}Zr(d,p)^{93}Zr$

Center-of-mass scattering angle, θ_{cm}, deg	Differential cross section, $\frac{d\sigma}{d\Omega}$, mb/sr	Statistical error of differential cross section, $\pm\Delta\frac{d\sigma}{d\Omega}$, mb/sr	Center-of-mass scattering angle, θ_{cm}, deg	Differential cross section, $\frac{d\sigma}{d\Omega}$, mb/sr	Statistical error of differential cross section, $\pm\Delta\frac{d\sigma}{d\Omega}$, mb/sr
$^{92}Zr(d,p)^{93}Zr^{2.666}$			$^{92}Zr(d,p)^{93}Zr^{2.795}$		
25.34	8.40×10^{-2}	4.15×10^{-2}	15.21	2.62	5.69×10^{-2}
30.40	9.87	3.86	20.28	3.71	4.44×10^{-1}
40.52	1.29×10^{-1}	1.14	25.34	2.26	7.47×10^{-2}
50.62	2.00	1.33	30.40	1.59	2.49
55.66	1.06	1.20	35.46	1.13	1.79
60.70	1.17	1.15	40.52	9.74×10^{-1}	1.53
65.73	1.00	1.10	45.57	1.03	1.77
70.76	8.95×10^{-2}	7.38×10^{-3}	50.62	1.09	1.55
75.78	6.94	9.17	55.66	8.56×10^{-1}	1.60
80.79	8.85	4.72	60.70	7.47	1.58
85.80	9.73	6.06	65.73	4.69	1.04
90.81	6.17	3.83	70.76	3.44	7.18×10^{-3}
			75.78	3.06	7.93
			80.79	2.73	6.45
			85.80	3.05	5.79
			90.81	2.58	5.25
			95.80	2.05	4.61
			100.79	1.57	3.55
$^{92}Zr(d,p)^{93}Zr^{2.694}$			$^{92}Zr(d,p)^{93}Zr^{2.895}$		
20.28	5.95×10^{-2}	3.39×10^{-2}	35.46	8.01×10^{-2}	7.34×10^{-3}
25.34	9.65	4.05	40.52	1.14×10^{-1}	6.34
30.40	1.25×10^{-1}	3.91	45.57	9.93×10^{-2}	7.72
40.52	1.55	1.16	55.66	9.99	5.67
45.57	1.55	1.16	60.70	1.10×10^{-1}	8.90
55.66	7.54×10^{-2}	1.19	65.73	7.28×10^{-2}	5.24
60.70	9.27	1.17	70.76	6.49	4.96
65.73	5.98	1.09	75.78	6.24	5.73
70.76	5.68	7.31×10^{-3}	80.79	5.02	3.86
75.78	7.34	9.36	85.80	5.30	3.44
80.79	3.51	4.12	90.81	4.10	2.59
90.81	2.46	3.52	95.80	2.75	2.19
95.80	3.65	3.02	100.79	2.17	1.36
100.79	2.90	1.52			

TABLE I. - Continued. DIFFERENTIAL CROSS SECTIONS FOR LEVELS INDUCED BY REACTION $^{92}Zr(d,p)^{93}Zr$

Center-of-mass scattering angle, θ_{cm}, deg	Differential cross section, $\frac{d\sigma}{d\Omega}$, mb/sr	Statistical error of differential cross section, $\pm\Delta\frac{d\sigma}{d\Omega}$, mb/sr	Center-of-mass scattering angle, θ_{cm}, deg	Differential cross section, $\frac{d\sigma}{d\Omega}$, mb/sr	Statistical error of differential cross section, $\pm\Delta\frac{d\sigma}{d\Omega}$, mb/sr
$^{92}Zr(d,p)^{93}Zr^{2.936}$			$^{92}Zr(d,p)^{93}Zr^{3.077}$		
15.21	9.74×10^{-2}	1.11×10^{-2}	15.21	2.47×10^{-2}	8.63×10^{-3}
20.28	1.32×10^{-1}	1.95	20.28	3.39	1.33×10^{-2}
35.46	9.12×10^{-2}	7.55×10^{-3}	25.34	1.13×10^{-1}	1.66
40.52	1.16×10^{-1}	6.34	30.40	9.74×10^{-2}	7.03×10^{-3}
45.57	8.12×10^{-2}	7.45	35.46	2.31×10^{-1}	1.31×10^{-2}
55.66	4.81	5.01	40.52	1.05	6.18×10^{-3}
60.70	5.77	7.90	45.57	4.98×10^{-2}	5.82
65.73	3.92	4.71	50.62	2.26	4.97
70.76	3.23	4.63	60.70	3.24	4.89
75.78	3.67	5.35	65.73	2.06	3.04
80.79	3.17	3.53	70.76	2.88	2.82
85.80	2.63	3.23	75.78	2.77	3.25
90.81	1.49	2.22	80.79	2.84	2.59
95.80	1.77	2.07	85.80	2.30	2.02
100.79	1.29	1.28	95.80	7.28×10^{-3}	1.36
			100.79	7.75	1.04
$^{92}Zr(d,p)^{93}Zr^{3.022}$			$^{92}Zr(d,p)^{93}Zr^{3.146}$		
20.28	2.74×10^{-1}	2.16×10^{-2}	15.21	1.97×10^{-1}	1.56×10^{-2}
25.34	3.53	2.49	20.28	1.98	1.95
30.40	4.94	1.22	25.34	2.28	2.18
40.52	4.83	1.06	30.40	1.18	7.03×10^{-3}
45.57	3.77	1.00	35.46	1.01	5.91
50.62	3.18	7.82×10^{-3}	45.57	6.72×10^{-2}	5.28
60.70	2.34	8.15	50.62	7.19	4.24
65.73	2.12	6.39	55.66	5.67	4.23
70.76	1.93	5.23	65.73	4.42	3.67
75.78	1.97	6.30	70.76	2.33	2.48
80.79	1.54	4.72	75.78	2.22	2.67
85.80	1.32	3.64	80.79	2.14	2.06
90.81	8.82×10^{-2}	2.84	85.80	2.41	1.95
95.80	6.61	2.48	90.81	1.99	1.73
100.79	5.68	2.13	95.80	2.46	1.60
			100.79	1.53	1.12

TABLE I. - Continued. DIFFERENTIAL CROSS SECTIONS FOR LEVELS INDUCED BY REACTION $^{92}Zr(d,p)^{93}Zr$

Center-of-mass scattering angle, θ_{cm}, deg	Differential cross section, $\frac{d\sigma}{d\Omega}$, mb/sr	Statistical error of differential cross section, $\pm\Delta\frac{d\sigma}{d\Omega}$, mb/sr	Center-of-mass scattering angle, θ_{cm}, deg	Differential cross section, $\frac{d\sigma}{d\Omega}$, mb/sr	Statistical error of differential cross section, $\pm\Delta\frac{d\sigma}{d\Omega}$, mb/sr
$^{92}Zr(d,p)^{93}Zr^{3.209}$			$^{92}Zr(d,p)^{93}Zr^{3.363}$		
15.21	2.65×10^{-1}	1.81×10^{-2}	15.21	1.91×10^{-1}	1.53×10^{-2}
20.28	1.87	2.05	20.28	1.29	1.95
25.34	1.47	2.07	25.34	2.39	2.49
30.40	1.07	8.23×10^{-3}	30.40	1.82	9.26×10^{-3}
35.46	1.02	6.53	35.46	1.45	7.34
40.52	1.24	5.69	40.52	1.42	6.51
50.62	6.22×10^{-2}	4.40	45.57	8.72×10^{-2}	6.36
55.66	3.83	4.01	60.70	5.09	6.02
70.76	2.91	2.68	70.76	3.96	3.15
75.78	2.51	2.87	75.78	3.93	3.53
80.79	2.40	2.13	80.79	3.81	2.66
85.80	2.70	2.02	85.80	3.50	2.43
90.81	1.82	1.73	90.81	1.70	2.04
95.80	1.92	1.48	95.80	1.84	1.66
100.79	1.61	1.13	100.79	1.21	1.12
$^{92}Zr(d,p)^{93}Zr^{3.297}$			$^{92}Zr(d,p)^{93}Zr^{3.421}$		
15.21	4.03×10^{-1}	2.23×10^{-2}	15.21	7.63×10^{-1}	3.07×10^{-2}
20.28	3.05	2.46	20.28	7.43	3.69
25.34	2.62	2.39	25.34	7.84	4.05
30.40	1.46	8.23×10^{-3}	30.40	6.92	1.58
35.46	1.05	6.53	35.46	5.70	1.28
40.52	1.05	5.53	40.52	4.52	1.04
45.57	1.18	7.85	45.57	3.39	1.04
50.62	1.01	5.38	50.62	3.40	8.23×10^{-3}
60.70	9.98×10^{-2}	6.40	55.66	2.67	7.90
65.73	3.89	6.49	60.70	3.08	1.04×10^{-2}
70.76	2.72	2.75	65.73	3.87	9.95×10^{-3}
75.78	2.87	3.06	70.76	1.46	4.90
80.79	2.73	2.26	75.78	1.19	5.16
85.80	3.18	2.16	80.79	9.09×10^{-2}	3.66
90.81	2.13	1.85	85.80	9.88	3.44
95.80	1.61	1.48	90.81	8.62	3.21
100.79	1.60	1.13	95.80	7.78	2.72
			100.79	7.11	2.38

TABLE I. - Continued. DIFFERENTIAL CROSS SECTIONS FOR LEVELS INDUCED BY REACTION $^{92}Zr(d,p)^{93}Zr$

Center-of-mass scattering angle, θ_{cm}, deg	Differential cross section, $\frac{d\sigma}{d\Omega}$, mb/sr	Statistical error of differential cross section, $\pm\Delta\frac{d\sigma}{d\Omega}$, mb/sr	Center-of-mass scattering angle, θ_{cm}, deg	Differential cross section, $\frac{d\sigma}{d\Omega}$, mb/sr	Statistical error of differential cross section, $\pm\Delta\frac{d\sigma}{d\Omega}$, mb/sr
$^{92}Zr(d,p)^{93}Zr^{3.486}$			$^{92}Zt(d,p)^{93}Zr^{3.649}$		
15.21	1.42×10^{-1}	1.32×10^{-2}	20.29	1.56×10^{-1}	1.74×10^{-2}
20.28	1.14	1.95	25.36	1.19	1.45
25.34	1.36	2.28	30.43	8.49×10^{-2}	2.23
30.40	9.87×10^{-2}	8.57×10^{-3}	35.49	9.49	7.33×10^{-3}
35.46	9.12	6.53	40.55	8.21	6.01
40.52	1.17×10^{-1}	6.18	45.60	5.85	5.54
45.57	4.41×10^{-2}	6.77	50.65	6.14	3.82
50.62	5.27	5.29	55.70	3.49	4.56
60.70	2.02	6.77	70.80	3.38	9.18
70.76	1.95	3.22			
75.78	2.85	3.63			
80.79	2.61	2.59			
85.80	2.09	2.16			
95.80	1.20×10^{-2}	1.54			
100.79	8.95×10^{-3}	1.04			
$^{92}Zr(d,p)^{93}Zr^{3.576}$			$^{92}Zr(d,p)^{93}Zr^{3.730}$		
15.22	1.37×10^{-1}	1.72×10^{-2}	15.22	4.54×10^{-1}	2.83×10^{-2}
20.29	1.48	1.64	20.29	5.70	2.97
25.36	1.87	1.66	25.36	5.33	3.11
30.43	1.10	1.06	30.43	2.61	1.10
35.49	1.01	7.95×10^{-3}	35.49	2.14	1.06
40.55	8.52×10^{-2}	6.18	40.55	1.55	8.13×10^{-3}
45.60	5.76	5.54	45.60	1.42	7.84
50.65	7.00	3.99	50.65	1.38	5.45
60.74	5.16	7.14	55.70	1.00	6.34
65.77	3.88	3.04	60.74	1.32	8.14
			65.77	8.75×10^{-2}	8.06
			70.80	7.72	4.69

TABLE I. - Continued. DIFFERENTIAL CROSS SECTIONS FOR LEVELS INDUCED BY REACTION $^{92}Zr(d,p)^{93}Zr$

Center-of-mass scattering angle, θ_{cm}, deg	Differential cross section, $\frac{d\sigma}{d\Omega}$, mb/sr	Statistical error of differential cross section, $\pm\Delta\frac{d\sigma}{d\Omega}$, mb/sr	Center-of-mass scattering angle, θ_{cm}, deg	Differential cross section, $\frac{d\sigma}{d\Omega}$, mb/sr	Statistical error of differential cross section, $\pm\Delta\frac{d\sigma}{d\Omega}$, mb/sr
$^{92}Zr(d,p)^{93}Zr^{3.821}$			$^{92}Zr(d,p)^{93}Zr^{3.966}$		
15.22	3.95×10^{-1}	2.58×10^{-2}	15.22	3.04×10^{-1}	3.20×10^{-2}
20.29	5.27	2.87	20.29	3.08	2.77
25.36	5.52	3.01	25.36	3.44	2.49
35.49	3.29	1.39	30.43	3.20	1.35
40.55	2.64	1.15	35.49	2.53	1.81
45.60	1.89	9.46×10^{-3}	40.55	2.10	1.22
50.65	1.71	6.27	45.60	1.72	1.03
55.70	1.52	8.00	50.65	1.34	6.51×10^{-3}
60.74	1.85	1.03×10^{-2}	55.70	9.91×10^{-2}	7.89
65.77	1.63	6.91×10^{-3}	60.74	1.07×10^{-1}	1.05×10^{-2}
70.80	1.05	5.23	65.77	8.98×10^{-2}	5.24×10^{-3}
			70.80	8.61	8.38
$^{92}Zr(d,p)^{93}Zr^{3.915}$			$^{92}Zr(d,p)^{93}Zr^{4.017}$		
15.22	2.60×10^{-1}	2.83×10^{-2}	15.22	1.59×10^{-1}	3.69×10^{-2}
20.29	2.40	2.56	20.29	2.22	2.87
25.36	2.52	2.18	35.49	2.41	1.73
30.43	2.73	1.27	45.60	1.67	1.65
40.55	1.69	1.06	50.65	1.25	8.22×10^{-3}
45.60	1.52	9.73×10^{-3}	55.70	9.20×10^{-2}	8.45
50.65	1.16	6.27	60.74	9.07	9.27
55.70	8.71×10^{-2}	8.56	65.77	7.07	5.55
60.74	1.11×10^{-1}	1.23×10^{-2}	70.80	6.58	5.83
65.77	7.30×10^{-2}	4.71×10^{-3}			

TABLE I. - Continued. DIFFERENTIAL CROSS SECTIONS FOR LEVELS INDUCED BY REACTION $^{92}Zr(d,p)^{93}Zr$

Center-of-mass scattering angle, θ_{cm}, deg	Differential cross section, $\frac{d\sigma}{d\Omega}$, mb/sr	Statistical error of differential cross section, $\pm\Delta\frac{d\sigma}{d\Omega}$, mb/sr	Center-of-mass scattering angle, θ_{cm}, deg	Differential cross section, $\frac{d\sigma}{d\Omega}$, mb/sr	Statistical error of differential cross section, $\pm\Delta\frac{d\sigma}{d\Omega}$, mb/sr
$^{92}Zr(d,p)^{93}Zr^{4.061}$			$^{92}Zr(d,p)^{93}Zr^{4.282}$		
15.22	4.26×10^{-1}	4.31×10^{-2}	15.22	1.26×10^{-1}	2.09×10^{-2}
20.29	4.41	3.38	20.29	1.43	1.85
25.36	5.75	3.11	30.43	1.32×10^{-1}	9.76×10^{-3}
30.43	5.57	1.73	35.49	1.13	1.14×10^{-2}
35.49	4.18	2.12	40.55	8.86×10^{-2}	7.48×10^{-3}
40.55	3.62	1.98	45.60	6.68	6.62
45.60	2.79	1.88	50.65	4.91	4.80
50.65	2.34	1.00	55.70	3.32	5.22
55.70	2.11	1.14	60.74	5.15	6.14
60.74	2.18	1.32	65.77	3.08	1.56×10^{-2}
65.77	1.61	6.91×10^{-3}	70.80	1.68	1.27×10^{-3}
70.80	1.27	7.37			
$^{92}Zr(d,p)^{93}Zr^{4.141}$			$^{92}Zr(d,p)^{93}Zr^{4.427}$		
15.22	1.42×10^{-1}	2.09×10^{-2}	15.22	1.39×10^{-1}	2.22×10^{-2}
20.29	1.86	2.05	20.29	1.44	1.95
25.36	1.94	1.87	25.36	1.39	1.97
30.43	1.82	1.04	30.43	1.47	1.03
35.49	1.59	1.10	35.49	1.27	1.10
40.55	1.50	8.78×10^{-3}	40.55	9.70×10^{-2}	7.96×10^{-3}
50.65	8.00×10^{-2}	4.88	45.60	9.11	7.30
55.70	7.34	5.89	50.65	7.29	4.96
60.74	7.28	6.51	55.70	7.69	6.11
65.77	6.22	3.88	60.74	7.20	7.64
70.80	5.61	4.09	65.77	4.79	3.77
			70.80	4.38	3.62

TABLE I. - Concluded. DIFFERENTIAL CROSS SECTIONS FOR LEVELS INDUCED BY REACTION $^{92}Zr(d,p)^{93}Zr$

Center-of-mass scattering angle, θ_{cm}, deg	Differential cross section, $\frac{d\sigma}{d\Omega}$, mb/sr	Statistical error of differential cross section, $\pm\Delta\frac{d\sigma}{d\Omega}$, mb/sr	Center-of-mass scattering angle, θ_{cm}, deg	Differential cross section, $\frac{d\sigma}{d\Omega}$, mb/sr	Statistical error of differential cross section, $\pm\Delta\frac{d\sigma}{d\Omega}$, mb/sr
$^{92}Zr(d,p)^{93}Zr^{4.716}$			$^{92}Zr(d,p)^{93}Zr^{4.840}$		
15.22	1.97×10^{-1}	2.95×10^{-2}	15.22	3.59×10^{-1}	3.57×10^{-2}
20.29	2.01	2.46	20.29	3.03	3.08
25.36	1.43	2.28	25.36	3.70	3.01
30.43	1.65	1.71	30.43	3.43	1.66
35.49	1.29	1.10	35.49	2.83	1.53
40.55	1.18	9.43×10^{-3}	40.55	2.55	1.37
45.60	1.03	8.24	45.60	2.17	1.31
50.65	8.26×10^{-2}	5.45	50.65	1.63	7.32×10^{-3}
55.70	7.64	6.34	55.70	1.28	8.34
60.74	6.80	7.52	60.74	1.34	1.01×10^{-2}
65.77	5.65	4.40	65.77	9.35×10^{-2}	5.66×10^{-3}
70.80	5.07	5.56	70.80	8.11	5.49
$^{92}Zr(d,p)^{93}Zr^{4.785}$					
30.43	8.73×10^{-2}	1.30×10^{-2}			
35.49	9.68	1.10			
40.55	6.89	9.43×10^{-3}			
45.60	7.22	1.05×10^{-2}			
50.65	4.26	5.21×10^{-3}			
55.70	2.89	5.89			
60.74	3.29	7.39			
65.77	2.79	4.29			

TABLE II. - DIFFERENTIAL CROSS SECTIONS FOR LEVELS INDUCED BY REACTION $^{92}Zr(d,t)^{91}Zr^{*}$

Center-of-mass scattering angle, θ_{cm}, deg	Differential cross section, $\frac{d\sigma}{d\Omega}$, mb/sr	Statistical error of differential cross section, $\pm\Delta\frac{d\sigma}{d\Omega}$, mb/sr	Center-of-mass scattering angle, θ_{cm}, deg	Differential cross section, $\frac{d\sigma}{d\Omega}$, mb/sr	Statistical error of differential cross section $\pm\Delta\frac{d\sigma}{d\Omega}$, mb/sr
$^{92}Zr(d,t)^{91}Zr^{g.s.}$			$^{92}Zr(d,t)^{91}Zr^{1.461}$		
15.47	2.30	9.89×10^{-2}	15.47	4.77×10^{-3}	3.57×10^{-3}
20.62	3.04	1.28×10^{-1}	20.62	9.94	3.97
25.77	2.57	1.14	25.77	1.31×10^{-2}	4.02
30.91	1.77	3.58×10^{-2}	30.91	7.98×10^{-3}	1.33
36.05	1.74	1.86	36.05	4.96	9.92×10^{-4}
41.17	1.91	3.34	41.17	6.02	1.11×10^{-3}
46.29	1.63	2.32	46.29	5.02	9.25×10^{-4}
51.40	1.04	1.71	51.40	4.78	7.17
56.49	7.74×10^{-1}	1.81	56.49	6.22	8.73
61.58	8.37	2.11	61.58	5.55	8.63
66.65	7.75	1.69	66.65	3.82	7.23
71.71	6.69	1.24	71.71	2.25	4.64
76.76	5.33	1.32	76.76	2.65	5.68
81.80	3.57	8.99×10^{-3}	81.80	2.18	4.63
86.82	2.81	6.52	86.82	2.22	4.03
91.82	2.24	7.17	91.82	2.16	4.32
$^{92}Zr(d,t)^{92}Zr^{1.196}$			$^{92}Zr(d,t)^{91}Zr^{1.876}$		
15.47	1.75×10^{-1}	1.67×10^{-2}	25.77	2.01×10^{-3}	3.02×10^{-3}
20.62	2.27	1.69	30.91	3.16	8.32×10^{-4}
25.77	2.39	1.81	51.40	2.79	6.38×10^{-4}
30.91	1.41	5.49×10^{-3}	61.58	2.59	6.16
36.05	9.00×10^{-2}	4.23	66.65	1.34	5.16
41.17	1.30×10^{-1}	4.91	71.71	1.79	3.98
46.29	1.86	5.15	76.76	2.08	4.73
51.40	1.59	4.22	81.80	1.65	3.97
56.49	1.19	4.36	86.82	1.81	3.49
61.58	7.17×10^{-2}	3.33	91.82	8.03×10^{-4}	3.09
66.65	4.12	2.27			
71.71	3.55	1.66			
76.76	4.49	2.27			
81.80	3.68	1.72			
86.82	3.67	1.68			
91.82	2.40	1.36			

TABLE II. - Continued. DIFFERENTIAL CROSS SECTIONS FOR LEVELS INDUCED BY REACTION $^{92}Zr(d,t)^{91}Zr^*$

Center-of-mass scattering angle, θ_{cm}, deg	Differential cross section, $\frac{d\sigma}{d\Omega}$, mb/sr	Statistical error of differential cross section, $\pm\Delta\frac{d\sigma}{d\Omega}$, mb/sr	Center-of-mass scattering angle, θ_{cm}, deg	Differential cross section, $\frac{d\sigma}{d\Omega}$, mb/sr	Statistical error of differential cross section, $\pm\Delta\frac{d\sigma}{d\Omega}$, mb/sr
$^{92}Zr(d,t)^{91}Zr^{2.036}$			$^{92}Zr(d,t)^{91}Zr^{2.186}$		
15.47	7.63×10^{-2}	1.07×10^{-2}	25.83	7.01×10^{-3}	4.01×10^{-3}
20.62	7.35	8.94×10^{-3}	30.91	9.32	1.83
25.77	7.54	9.05	36.05	1.27×10^{-2}	1.59
30.91	6.49	3.49	41.17	1.17	1.43
36.05	5.18	3.20	46.29	8.32×10^{-3}	1.19
41.17	3.74	2.53	51.40	7.41	9.57×10^{-4}
46.29	3.75	2.25	56.49	5.46	1.20×10^{-3}
51.40	3.29	1.75	61.58	6.29	1.11
56.49	3.00	1.96	66.65	5.47	1.24
61.58	3.30	2.22	71.71	5.76	1.06
66.65	2.59	1.76	81.80	5.62	1.59
			86.82	4.10	7.39×10^{-4}
			91.82	4.57	8.65
$^{92}Zr(d,t)^{91}Zr^{2.127}$			$^{92}Zr(d,t)^{91}Zr^{2.350}$		
25.83	2.50×10^{-2}	6.01×10^{-3}	15.51	4.86×10^{-2}	8.31×10^{-3}
30.91	3.69	2.83	20.67	4.35	6.93
36.05	4.10	2.85	25.83	3.80	6.17
41.17	4.36	2.85	30.91	3.66	2.66
46.29	4.03	2.38	36.05	4.94	3.13
51.40	4.18	2.07	41.17	5.70	3.17
56.49	4.06	2.40	46.29	4.61	2.51
61.58	4.28	2.59	51.40	3.99	1.91
66.65	3.48	2.27	56.49	3.07	2.18
71.71	2.84	1.66	61.58	3.14	2.10
76.76	2.35	2.37	66.65	2.76	1.86
81.80	2.03	1.45	71.71	2.79	1.46
86.82	2.13	1.34	76.76	2.51	1.61
91.82	1.65	1.30	81.80	2.30	1.32
			86.82	2.22	1.28
			91.82	2.04	1.30

TABLE II. - Continued. DIFFERENTIAL CROSS SECTIONS FOR LEVELS INDUCED BY REACTION $^{92}Zr(d,t)^{91}Zr^*$

Center-of-mass scattering angle, θ_{cm}, deg	Differential cross section, $\frac{d\sigma}{d\Omega}$, mb/sr	Statistical error of differential cross section, $\pm\Delta\frac{d\sigma}{d\Omega}$, mb/sr	Center-of-mass scattering angle, θ_{cm}, deg	Differential cross section, $\frac{d\sigma}{d\Omega}$, mb/sr	Statistical error of differential cross section, $\pm\Delta\frac{d\sigma}{d\Omega}$, mb/sr
$^{92}Zr(d,t)^{91}Zr^{2.817}$			$^{92}Zr(d,t)^{91}Zr^{3.045}$		
25.83	5.01×10^{-3}	2.24×10^{-3}	15.51	3.56×10^{-3}	2.37×10^{-3}
31.02	5.79	1.16	31.02	2.98	9.92×10^{-4}
36.17	2.96	1.18	36.17	3.15	9.85
41.31	3.94	1.10	41.31	3.94	9.45
46.44	5.26	1.05	46.44	2.50	1.05×10^{-3}
51.56	4.92	8.72×10^{-4}	51.56	2.06	7.93×10^{-4}
56.67	3.80	8.69	56.67	3.37	1.09×10^{-3}
61.77	3.56	9.83	71.92	2.45	9.92×10^{-4}
66.85	2.57	9.26	76.97	3.02	6.61
76.97	2.46	6.61			
82.01	2.84	5.29			
$^{92}Zr(d,t)^{91}Zr^{2.896}$			$^{92}Zr(d,t)^{91}Zr^{3.100}$		
15.51	1.39×10^{-1}	1.28×10^{-2}	20.73	9.84×10^{-3}	3.94×10^{-3}
20.67	1.53	2.08	25.90	6.97	2.99
25.83	1.50	1.90	31.02	9.26	1.65
31.02	1.53	8.60×10^{-3}	36.17	8.67	1.38
36.17	1.46	7.09	41.31	1.02×10^{-2}	1.42
41.31	1.55	6.46	46.44	1.04	7.36
46.44	1.70	7.75	51.56	8.25×10^{-3}	1.11
51.56	1.86	6.74	56.67	8.37	1.41
56.67	2.02	8.04	61.77	7.49	1.11
61.77	2.17	8.48	66.85	8.54	1.24
66.85	1.82	7.82	71.92	6.81	1.19
71.92	1.33	3.97	76.97	6.33	8.50×10^{-4}
76.97	1.11	5.38	82.01	5.95	7.93
82.01	8.73×10^{-2}	4.03			

TABLE II. - Continued. DIFFERENTIAL CROSS SECTIONS FOR LEVELS INDUCED BY REACTION $^{92}Zr(d,t)^{91}Zr^*$

Center-of-mass scattering angle, θ_{cm}, deg	Differential cross section, $\frac{d\sigma}{d\Omega}$, mb/sr	Statistical error of differential cross section, $\pm\Delta\frac{d\sigma}{d\Omega}$, mb/sr	Center-of-mass scattering angle, θ_{cm}, deg	Differential cross section, $\frac{d\sigma}{d\Omega}$, mb/sr	Statistical error of differential cross section, $\pm\Delta\frac{d\sigma}{d\Omega}$, mb/sr
$^{92}Zr(d,t)^{91}Zr$ 3.229			$^{92}Zr(d,t)^{91}Zr$ 3.468		
15.55	6.61×10^{-2}	8.83×10^{-3}	15.55	4.37×10^{-2}	7.18×10^{-3}
20.73	6.10	1.08×10^{-2}	20.73	2.17	4.92
25.90	7.57	1.10	25.90	3.09	5.98
31.02	5.97	4.13×10^{-3}	31.02	3.50	2.98
36.17	7.19	4.34	36.17	4.39	5.12
41.31	6.38	3.47	41.31	4.32	2.84
46.44	5.62	3.42	46.44	3.69	2.63
51.56	5.53	2.70	51.56	3.17	1.90
56.67	6.14	3.26	56.67	3.74	2.39
61.77	7.21	3.69	61.77	3.80	2.46
66.85	6.03	3.29	66.85	3.58	2.37
71.92	4.91	2.05	71.92	3.40	1.59
76.97	4.64	2.74	76.97	3.37	2.27
82.01	3.53	2.05	82.01	2.90	1.78
$^{92}Zr(d,t)^{91}Zr$ 3.314			$^{92}Zr(d,t)^{91}Zr$ 3.568		
20.73	4.92×10^{-3}	6.89×10^{-3}	15.55	2.95×10^{-2}	5.90×10^{-3}
25.90	7.97	2.99	20.73	3.84	7.87
31.02	7.44	2.98	31.02	4.64	3.47
36.17	5.71	1.18	36.17	4.89	3.35
41.31	5.20	9.45×10^{-4}	41.31	4.49	2.99
46.44	5.91	1.71×10^{-3}	46.44	3.76	2.76
51.56	6.58	9.52×10^{-4}	51.56	3.36	2.06
56.67	1.02×10^{-2}	1.20×10^{-3}	56.67	3.44	4.67
61.77	9.09×10^{-3}	1.11	61.77	4.57	3.32
66.85	6.59	9.26×10^{-4}	66.85	4.06	2.57
71.92	6.15	7.27	71.92	3.39	2.65
76.97	3.87	1.61×10^{-3}	76.97	3.55	2.27
82.01	2.25	5.95×10^{-4}	82.01	3.24	1.92

TABLE II. - Continued. DIFFERENTIAL CROSS SECTIONS FOR LEVELS INDUCED BY REACTION $^{92}Zr(d,t)^{91}Zr^*$

Center-of-mass scattering angle, θ_{cm}, deg	Differential cross section, $\frac{d\sigma}{d\Omega}$, mb/sr	Statistical error of differential cross section, $\pm\Delta\frac{d\sigma}{d\Omega}$, mb/sr	Center-of-mass scattering angle, θ_{cm}, deg	Differential cross section, $\frac{d\sigma}{d\Omega}$, mb/sr	Statistical error of differential cross section, $\pm\Delta\frac{d\sigma}{d\Omega}$, mb/sr
$^{92}Zr(d,t)^{91}Zr^{3.695}$			$^{92}Zr(d,t)^{91}Zr^{3.891}$		
15.55	3.54×10^{-3}	2.36×10^{-3}	15.55	3.19×10^{-2}	6.13×10^{-3}
20.73	7.87	2.95	20.73	2.46	5.90
25.90	9.96	3.98	25.90	3.88	7.97
31.02	9.59	2.48	31.02	2.76	2.64
36.17	1.04×10^{-2}	2.36	36.17	2.36	2.36
46.44	7.75×10^{-3}	2.10	41.31	2.76	2.52
51.56	9.12	1.74	46.44	3.19	2.63
56.67	1.12×10^{-2}	1.85	51.56	3.52	2.14
61.77	1.08	1.60	56.67	4.11	2.61
66.85	7.21×10^{-3}	2.26	61.77	3.78	2.70
71.92	8.13	8.60×10^{-4}	66.85	3.50	2.37
76.97	6.33	2.36×10^{-3}	71.92	2.67	1.52
			76.97	2.30	1.79
			82.01	1.87	1.39
$^{92}Zr(d,t)^{91}Zr^{3.739}$			$^{92}Zr(d,t)^{91}Zr^{3.952}$		
15.55	1.42×10^{-2}	4.09×10^{-3}	25.90	5.98×10^{-3}	5.98×10^{-3}
31.02	2.13	3.14	31.02	5.12	1.32
36.17	2.15	2.96	36.17	6.50	1.58
41.31	2.08	2.05	41.31	5.36	1.58
46.44	1.60	2.50	46.44	6.04	1.45
51.56	1.06	1.82	51.56	6.26	1.11
56.67	1.21	1.96	56.67	7.17	1.30
61.77	1.87	1.97	61.77	8.60	1.47
66.85	1.85	2.06	66.85	6.79	1.13
71.92	1.84	1.19	71.92	6.22	9.26×10^{-4}
76.97	1.35	2.83	76.97	5.57	8.50
82.01	9.71×10^{-3}	8.65			

TABLE II. - Concluded. DIFFERENTIAL CROSS SECTIONS FOR LEVELS INDUCED BY REACTION $^{92}Zr(d,t)^{91}Zr^*$

Center-of-mass scattering, angle, θ_{cm}, deg	Differential cross section, $\frac{d\sigma}{d\Omega}$, mb/sr	Statistical error of differential cross section, $\pm\Delta\frac{d\sigma}{d\Omega}$, mb/sr
$^{92}Zr(d,t)^{91}Zr^{4.005}$		
31.02	5.45×10^{-3}	1.32×10^{-3}
41.31	5.67	1.10
46.44	5.26	9.20×10^{-4}
51.56	3.73	8.72
56.67	3.59	9.78
61.77	2.70	8.60
66.85	3.29	7.21
71.92	3.57	6.61

TABLE III. - OPTICAL POTENTIALS USED IN DWBA DIRECT REACTION CALCULATIONS

[E = incident laboratory energy in MeV; Z = number of protons in target nucleus; N = number of neutrons in target nucleus; A = atom mass number of target nucleus.]

	Deuteron optical potential[a]	Proton optical potential[b]	Triton optical potential[c]	Bound-state potential
Real strength, MeV	94.7	$54 - 0.32E + 0.4\left(\frac{Z}{A^{1/3}}\right) + 24\left[\frac{(N-Z)}{A}\right]$	$165 - 0.17E - 6.4\left[\frac{(N-Z)}{A}\right]$	-----
Diffuseness of real potential, fm	0.802	0.75	0.72	0.67
Radius of real potential, fm	1.15	1.17	1.20	1.27
Central imaginary strength, MeV	------	0.22 E - 2.7, or zero, whichever is greater	$46 - 0.33E - 110\left[\frac{(N-Z)}{A}\right]$	-----
Surface imaginary strength, MeV	47.8	$11.8 - 0.25E + 12\left[\frac{(N-Z)}{A}\right]$, or zero, whichever is greater	----------	-----
Diffuseness of imaginary potential, MeV	0.841	$0.51 + 0.7\left[\frac{(N-Z)}{A}\right]$	0.84	-----
Radius of imaginary potential, fm	1.36	1.32	1.40	-----
Coulomb radius, fm	1.25	1.25	1.30	-----
Spin-orbit strength, MeV	------	----------	----------	32

[a]Determined from present work.
[b]Ref. 13.
[c]Ref. 14.

TABLE IV. - EXCITATION ENERGIES, MOMENTUM TRANSFERS, PARITIES AND POSSIBLE SPIN ASSIGNMENTS, AND SPECTROSCOPIC STRENGTH FACTORS FOR EXCITED LEVELS IN ^{93}Zr

[Reaction $^{92}Zr(d, p)^{93}Zr$.]

Excitation energy, MeV	Momentum transfer, Δl	Parity and possible spin assignment, J^{π}	Spectroscopic strength factor, S	Excitation energy, MeV	Momentum transfer, Δl	Parity and possible spin assignment, J^{π}	Spectroscopic strength factor, S
0.000	2	$5/2^+$	0.54	3.022	4	$(9/2, 7/2)^+$	0.14, 0.29
.260	(2)	$(5/2, 3/2)^+$	0.001, 0.003	3.077	0	$1/2^+$	0.018
.947	0	$1/2^+$	0.53	3.146	2	$(5/2, 3/2)^+$	0.009, 0.017
1.018	↓	↓	0.13	3.209	1	$(3/2, 1/2)^-$	0.007, 0.014
1.151	↓	↓	0.002	3.297	2	$(5/2, 3/2)^+$	0.013, 0.024
1.222	↓	↓	0.006	3.363	1	$(3/2, 1/2)^-$	0.008, 0.018
1.430	2	$(5/2, 3/2)^+$	0.20, 0.37	3.421	3	$(7/2, 5/2)^-$	0.046, 0.081
1.480	4	$(9/2, 7/2)^+$	0.21, 0.45	3.486	1	$(3/2, 1/2)^-$	0.005, 0.011
1.648	2	$(5/2, 3/2)^+$	0.017, 0.027	3.576	3	$(7/2, 5/2)^-$	0.008, 0.015
1.919	0	$1/2^+$	0.088	3.649	1	$(3/2, 1/2)^-$	0.006, 0.013
2.040	5	$(11/2, 9/2)^-$	0.27, 0.795	3.730	2	$(5/2, 3/2)^+$	0.021, 0.036
2.101	0	$1/2^+$	0.072	3.821	3	$(7/2, 5/2)^-$	0.026, 0.045
2.181				3.915	3	$(7/2, 5/2)^-$	0.014, 0.025
2.276				3.966	3	$(7/2, 5/2)^-$	0.016, 0.030
2.325	3	$(7/2, 5/2)^-$	0.007, 0.014	4.017	4	$(9/2, 7/2)^+$	0.048, 0.11
2.391	0	$1/2^+$	0.004	4.061	3	$(7/2, 5/2)^-$	0.029, 0.053
2.488	2	$(5/2, 3/2)^+$	0.11, 0.20	4.141	3	$(7/2, 5/2)^-$	0.009, 0.017
2.553	2	$(5/2, 3/2)^+$	0.045, 0.081	4.218			
2.666	5	$(11/2, 9/2)^-$	0.096, 0.28	4.282	3	$(7/2, 5/2)^-$	0.007, 0.012
2.694	4	$(9/2, 7/2)^+$	0.042, 0.093	4.427	3	$(7/2, 5/2)^-$	0.008, 0.013
2.795	2	$(5/2, 3/2)^+$	0.14, 0.26	4.618			
2.895	5	$(11/2, 9/2)^-$	0.061, 0.18	4.716	3	$(7/2, 5/2)^-$	0.008, 0.014
2.936	3	$(7/2, 5/2)^-$	0.009, 0.017	4.785	1	$(3/2, 1/2)^-$	0.004, 0.008
				4.840	3	$(7/2, 5/2)^-$	0.015, 0.027

TABLE V. - EXCITATION ENERGIES, MOMENTUM TRANSFERS, PARITIES AND SHELL MODEL SPIN ASSIGNMENTS, AND SPECTROSCOPIC STRENGTH FACTORS FOR EXCITED LEVELS IN ^{93}Zr COMPARED TO PREVIOUSLY REPORTED RESULTS

This work				Previous (d,p) work						Previous isobaric analog resonance study (ref. 2)			
				Reference 1			Reference 3			Elastic		Inelastic	
Excitation energy, MeV	Momentum transfer, Δl	Parity and possible spin assignment[a], J^π	Spectroscopic strength factor, S	Δl	J^π	S	Δl	J^π	S	J^π	S	[Coupling]$_{J^\pi}$	S
g.s.	2	$5/2^+$	0.54	2	$5/2^+$	0.54	2	$5/2^+$	0.55				
0.260	(2)	$(3/2, 5/2)^+$	0.003, 0.001										
0.947	0	$1/2^+$	0.53	0	$1/2^+$	0.91	0	$1/2^+$	0.70	$1/2^+$	0.54		
1.018			0.13										
1.151			0.002										
1.222			0.006									$\left[2_1^+ \times \nu(S_{1/2})\right]_{3/2^+}$	0.071
1.430	2	$3/2^+$	0.37	2	$3/2^+$	0.38	2	$3/2^+$	0.60	$3/2^+$	0.17	$\left[2_2^+ \times \nu(l_j)\right]_{3/2^+}$	
1.480	4	$7/2^+$	0.45									$\left[2_3^+ \times \nu(S_{1/2})\right]_{3/2^+}$	0.045
1.648	2	$(3/2, 5/2)^+$	0.027, 0.017	(4)	$(7/2)^+$	(0.11)	4	$7/2^+$					
1.919	0	$1/2^+$	0.088	0	$1/2^+$	0.21	0	$1/2^+$	0.13	$1/2^+$	0.09	$\left[0_2^+ \times \nu(S_{1/2})\right]_{1/2^+}$	0.047
												$\left[2_3^+ \times \nu(l_j)\right]_{1/2^+}$	
2.040	5	$11/2^-$	0.27	(4)	$(7/2)^+$	(0.42)	(5)	$(11/2)^-$	(0.20)				
2.101	0	$1/2^+$	0.072				(4)	$(7/2)^+$	(0.48)				
2.181													
2.276													
2.325	3	$7/2^-$	0.007	4	$7/2^+$	0.09	(4)	$(7/2)^+$					
2.391	0	$1/2^+$	0.004										
2.488	2	$3/2^+$	0.20	2	$3/2^+$	0.24	(2)	$(3/2)^+$	(0.25)			$\left[2_2^+ \times \nu(l_j)\right]_{3/2^+}$	
2.553	2	$3/2^+$	0.081				(2)	$(3/2)^+$	(0.08)			$\left[2_1^+ \times \nu(d_{3/2})\right]_{3/2^+}$	0.053
2.666	5	$11/2^-$	0.096				5	$11/2^-$	0.12				

2.694	4	$7/2^+$	0.093									$\left[2_1^+ \times \nu(d_{3/2})\right]_{3/2^+}$	0.089
2.795	2	$3/2^+$	0.26	2	$3/2^+$	0.21	(2)	$(3/2)^+$	(0.29)	$3/2^+$	0.15	$\left[0_2^+ \times \nu(d_{3/2})\right]_{3/2^+}$	0.034
2.895	5	$11/2^-$	0.061									$\left[2_2^+ \times \nu(S_{1/2})\right]_{3/2^+}$	0.038
												$\left[2_3^+ \times \nu(l_j)\right]_{3/2^+}$	
2.936	3	$7/2^-$	0.009										
3.022	4	$7/2^+$	0.29	4	$7/2^+$	0.30	4	$7/2^+$	0.37	$7/2^+$	0.24		
3.077	0	$1/2^+$	0.018										
3.146	2	$(3/2, 5/2)^+$	0.017, 0.009										
3.209	1	$3/2^-$	0.007	2	$3/2^+$	0.38	(2)	$(3/2)^+$					
3.297	2	$3/2^+$	0.024	2	$3/2^+$	0.028	(2)	$(3/2)^+$			≤ 0.024	$\left[0_2^+ \times \nu(d_{3/2})\right]_{3/2^+}$	≥ 0.26
3.363	1	$3/2^-$	0.008										
3.421	3	$7/2^-$	0.046	1	$3/2^-$	0.117	(3,2)		(~0.10)	$7/2^-$		$\left[0_2^+ \times \nu(f_{7/2})\right]_{7/2^-}$	
3.486	1	$3/2^-$	0.005									$\left[3^- \times \nu(l_j)\right]_{7/2^-}$	
3.576	3	$7/2^-$	0.008										
3.649	1	$3/2^-$	0.006										
3.730	2	$(3/2, 5/2)^+$	0.036, 0.021										
3.821	3	$7/2^-$	0.026										
3.915	3	$7/2^-$	0.014										
3.966	3	$7/2^-$	0.016										
4.017	4	$7/2^+$	0.11										
4.061	3	$7/2^-$	0.029										
4.141	3	$7/2^-$	0.009										
4.218													
4.282	3	$7/2^-$	0.007										
4.427	3	$7/2^-$	0.008										
4.618													
4.716	3	$7/2^-$	0.008										
4.785	1	$3/2^-$	0.004										
4.840	3	$7/2^-$	0.015										

[a]Assumed from shell model considerations.

TABLE VI. - EXCITATION ENERGIES, MOMENTUM TRANSFERS, PARATIES AND POSSIBLE SPIN ASSIGNMENTS, AND SPECTROSCOPIC STRENGTH FACTORS FOR EXCITED LEVELS IN ^{91}Zr

[Reaction $^{92}Zr(d,t)^{91}Zr$.]

Excitation energy, MeV	Momentum transfer, Δl	Parity and possible spin assignment, J^{π}	Spectroscopic strength factor, C^2S
0.000	2	$5/2^+$	1.49
1.196	(0)	$(1/2)^+$	0.10
1.277			
1.461	2	$(5/2, 3/2)^+$	0.014, 0.018
1.876	4	$(9/2, 7/2)^+$	0.052, 0.104
2.036	2	$(5/2, 3/2)^+$	0.18, 0.21
2.127	4	$(9/2, 7/2)^+$	0.63, 1.35
2.186	4	$(9/2, 7/2)^+$	0.14, 0.30
2.350	1	$(3/2, 1/2)^-$	0.18, 0.21
2.431			
2.766			
2.817	2	$(5/2, 3/2)^+$	0.030, 0.036
2.896	4	$(9/2, 7/2)^+$	4.68, 10.0
2.984			
3.045	(1)	$(3/2, 1/2)^-$	0.024, 0.028
3.100	4	$(9/2, 7/2)^+$	0.27, 0.60
3.229	1	$(3/2, 1/2)^-$	0.65, 0.77
3.314	0	$1/2^+$	0.06
3.468	1	$(3/2, 1/2)^-$	0.52, 0.62
3.568	1	$(3/2, 1/2)^-$	0.67, 0.79
3.695	4	$(9/2, 7/2)^+$	0.50, 1.10
3.739	1	$(3/2, 1/2)^-$	0.36, 0.44
3.818			
3.891	4	$(9/2, 7/2)^+$	2.21, 4.86
3.952	4	$(9/2, 7/2)^+$	0.44, 0.97
4.005	2	$(5/2, 3/2)^+$	0.098, 0.14

TABLE VII. - EXCITATION ENERGIES, MOMENTUM TRANSFERS, PARITIES AND SHELL MODEL SPIN ASSIGNMENTS, AND SPECTROSCOPIC STRENGTH FACTORS FOR EXCITED LEVELS IN ^{91}Zr COMPARED TO PREVIOUSLY REPORTED RESULTS

This work				Previous (p,d) work (ref. 7)				Previous (α,nγ) work (ref. 6)		Previous (d,t) work (ref. 1)		Previous (p,p') work (ref. 10)		Previous (d,p) work								
														Reference 4			Reference 5			Reference 1		
Excitation energy, MeV	Momentum transfer, Δl	Parity and possible spin assignment[a], J^π	Spectroscopic strength factor, C^2S	Excitation energy, MeV	Δl	J^π	C^2S	Excitation energy, MeV	J^π	J^π	C^2S	Excitation energy, MeV	J^π	Excitation energy, MeV	J^π	S	Excitation energy, MeV	J^π	(2J + 1)S	Excitation energy, MeV	J^π	S
0.000	2	$5/2^+$	1.49	0.000	2	$5/2^+$	1.86±0.33	0.000	$5/2^+$	$5/2^+$	1.56	0.000	$5/2^+$	0.000	$5/2^+$	1.04	0.000	$5/2^+$	5.7	0.000	$5/2^+$	0.89
1.196	0	$1/2^+$	0.10	1.204	0	$1/2^+$	0.06	1.205	$1/2^+$	$1/2^+$	0.15	1.21	$1/2^+$	1.201	$1/2^+$	0.93	1.204	$1/2^+$	1.31	1.21	$1/2^+$	0.72
1.277																						
1.461	2	$5/2^+$	0.014	1.47			(b)	1.466	$5/2^+$			1.46	$5/2^+$	1.459	$5/2^+$	0.03	1.468	$5/2^+$	0.14	1.48	$3/2^+$	0.029
1.876	4	$9/2^+$	0.052					1.882	$7/2^+$	$7/2^+$	0.05	1.876	$9/2^+$	1.871	$7/2^+$	0.08	1.883	$9/2^+$	0.61	1.89	$7/2^+$	0.062
2.036	2	$3/2^+$	0.21	2.04	2	$3/2^+$	0.07	2.041	$3/2^+$	$3/2^+$	0.10	2.035	$5/2^+$	2.031	$3/2^+$	0.63	2.040	$3/2^+$	2.20	2.06	$3/2^+$	0.45
2.127	4	$9/2^+$	0.63	2.185	4	$9/2^+$	0.78	2.132	$9/2^+$			2.123	$7/2^+$				2.127					
2.186	4	$7/2^+$	0.30	2.180	4	$7/2^+$	0.20	2.189	$(3/2,5/2)^+$	$7/2^+$	0.43	2.19	$7/2^+$	2.186	$7/2^+$	0.48	2.195	$7/2^+$	4.20	2.21	$7/2^+$	0.52
2.350	1	$(3/2,1/2)^-$	0.18,0.21	2.350				2.356	$(1/2)$								2.353			2.35	$(7/2)^+$	0.05
2.431																						
2.766								2.775	(3/2)													
2.817	2	$5/2^+$	0.030									2.821	$(5/2)^-$	2.792	$(3/2)^+$	(0.07)	2.807	$5/2^+$	0.15			
2.896	4	$9/2^+$	4.68	2.895	4	$9/2^+$	7.9	2.914	$(9/2)^+$					2.902	$(1/2)^+$	(0.10)	2.926					
2.984																						
3.045	(1)	$(3/2,1/2)^-$	0.024,0.028																			
3.100	4	$9/2^+$	0.27																			
3.229	1	$(3/2,1/2)^-$	0.65,0.77	3.225	1	$(1/2,3/2)^-$	1.00,0.91															
3.314	0	$1/2^+$	0.06														3.332	$1/2^+$	0.14			
3.468	1	$(3/2,1/2)^-$	0.52,0.62	3.468	1	$(1/2,3/2)^-$	0.82,0.76										3.462	$7/2^+$	3.6			
3.568	1	$(3/2,1/2)^-$	0.67,0.79	3.567	1	$(1/2,3/2)^-$	1.14,1.04															
3.695	4	$9/2^+$	0.50	3.695	4	$9/2^+$	0.45															
3.739	1	$(3/2,1/2)^-$	0.36,0.44	3.738	2	$(5/2,3/2)^+$	0.14,1.06										3.739	$(5/2,3/2)^+$	(0.05,0.06)			
3.818														3.824	$(3/2)^+$	(0.12)						
3.891	4	$9/2^+$	2.21	3.890	(3,4)												3.903					
3.952	4	$9/2^+$	0.44																			
4.005	2	$5/2^+$	0.098																			

[a]Assumed from shell model considerations.

[b]Very weak.

"The aeronautical and space activities of the United States shall be conducted so as to contribute . . . to the expansion of human knowledge of phenomena in the atmosphere and space. The Administration shall provide for the widest practicable and appropriate dissemination of information concerning its activities and the results thereof."

—NATIONAL AERONAUTICS AND SPACE ACT OF 1958

NASA SCIENTIFIC AND TECHNICAL PUBLICATIONS

TECHNICAL REPORTS: Scientific and technical information considered important, complete, and a lasting contribution to existing knowledge.

TECHNICAL NOTES: Information less broad in scope but nevertheless of importance as a contribution to existing knowledge.

TECHNICAL MEMORANDUMS: Information receiving limited distribution because of preliminary data, security classification, or other reasons.

CONTRACTOR REPORTS: Scientific and technical information generated under a NASA contract or grant and considered an important contribution to existing knowledge.

TECHNICAL TRANSLATIONS: Information published in a foreign language considered to merit NASA distribution in English.

SPECIAL PUBLICATIONS: Information derived from or of value to NASA activities. Publications include conference proceedings, monographs, data compilations, handbooks, sourcebooks, and special bibliographies.

TECHNOLOGY UTILIZATION PUBLICATIONS: Information on technology used by NASA that may be of particular interest in commercial and other non-aerospace applications. Publications include Tech Briefs, Technology Utilization Reports and Technology Surveys.

Details on the availability of these publications may be obtained from:

SCIENTIFIC AND TECHNICAL INFORMATION OFFICE

NATIONAL AERONAUTICS AND SPACE ADMINISTRATION

Washington, D.C. 20546